J. Fluid Mech. (2004), *vol.* 521, *pp.* 1–34.
DOI: 10.1017/S002211200400165X Printed in the United Kingdom

Gravity currents produced by lock exchange

By J. O. SHIN[1], S. B. DALZIEL[1] AND P. F. LINDEN[2]

[1] Department of Applied Mathematics and Theoretical Physics, University of Cambridge, Wilberforce Road, Cambridge CB3 0WA, UK

[2] Department of Mechanical and Aerospace Engineering, University of California, San Diego, 9500 Gilman Drive, La Jolla, CA 92093-0411, USA

(Received 5 April 2002 and in revised form 17 May 2004)

The dynamics of gravity currents are believed to be strongly influenced by dissipation due to turbulence and mixing between the current and the surrounding ambient fluid. This paper describes new theory and experiments on gravity currents produced by lock exchange which suggest that dissipation is unimportant when the Reynolds number is sufficiently high. Although there is mixing, the amount of energy dissipated is small, reducing the current speed by a few percent from the energy-conserving value. Benjamin (*J. Fluid Mech.* vol. 31, 1968, p. 209) suggests that dissipation is an essential ingredient in gravity current dynamics. We show that dissipation is not important at high Reynolds number, and provide an alternative theory that predicts the current speed and depth based on energy-conserving flow that is in good agreement with experiments. We predict that in a deep ambient the front Froude number is 1, rather than the previously accepted value of $\sqrt{2}$. New experiments are reported for this case that support the new theoretical value.

1. Introduction

This paper provides an analysis of the motion of a gravity current produced by lock exchange. In a lock exchange experiment, fluids of different densities initially at rest are separated by a vertical barrier – the lock gate – in a tank. When the gate is removed, differences in the hydrostatic pressure cause the denser fluid to flow in one direction along the bottom boundary of the tank, while the lighter fluid flows in the opposite direction along the top boundary of the tank. Figure 1 shows the initial configurations for lock exchange flows: a *full-depth* release when the depths of heavy and light fluid on both sides of the gate are equal is shown in (*a*) and a *partial-depth* release when the dense fluid occupies only a fraction of the full depth is shown in (*b*).

Figure 2 shows the flow resulting from a full-depth lock release experiment. In this case the densities on the two sides of the lock gate are very similar (the density ratio $\gamma = \rho_1/\rho_2 < 1$ is close to unity). A dense gravity current travels to the right along the lower boundary and a buoyant current travels to the left along the upper boundary. Visually the flows are very nearly symmetric, and the dense and light fronts travel at almost the same speeds (figure 2*b*). The currents occupy about half the channel depth in each case, although they may be shallower immediately behind the head where there is mixing.

The speeds of the two currents are constant within experimental resolution. Previous similar observations led Benjamin (1968) to develop a theory for the propagation of a steadily advancing current. He considered one half of the flow shown in figure 2(*a*), say the dense current only. In a frame of reference moving with the current, the front

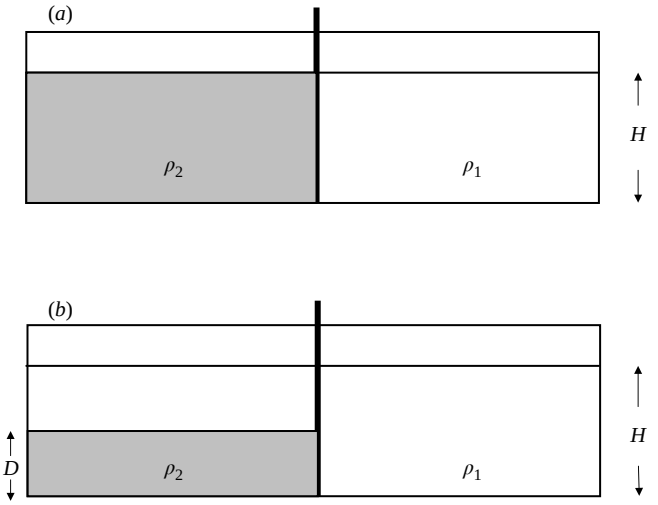

FIGURE 1. A schematic of the lock release initial conditions. The flow is started by removing the gate vertically. The dense fluid $\rho_2 > \rho_1$ occupies the depth H in a full-depth release (a) and a depth $D < H$ in a partial depth release (b). For complete symmetry in the full-depth release the upper boundary should be rigid, as is the case in figure 2.

is at rest and it is possible to develop a hydraulic theory which equates the fluxes of mass and momentum into and out of a control volume bounded by the upper and lower boundaries of the channel, and vertical planes upstream and downstream of the front. Benjamin showed that there was a range of possible solutions depending on the depth of the current, and a further condition is needed to determine the depth of the current. Benjamin (1968) showed that if he assumed that the energy fluxes into and out of this volume were also the same, these solutions reduced to two cases. The first is when the depth of the current is zero and the second is when the current occupied exactly one-half the depth. This latter solution is close to the depth seen in figure 2, and the speed predicted in this case is very close to that found from the data in figure 2(b). So, despite the mixing clearly visible in the shadowgraph images and other dissipation due to turbulence and viscous stresses, a theory which assumes conservation of energy seems to describe the experiments satisfactorily.

Early evidence for the existence of half-depth, energy-conserving currents was provided by Gardner & Crow (1970) and Wilkinson (1982), who carried out experiments with air cavities intruding into a water-filled channel. When surface tension effects were small, they observed that the cavities could occupy half the depth and that the free surface was smooth implying almost no loss of energy, consistent with Benjamin's energy-conserving theory. In fact, as we discuss below, the theory by Benjamin (1968) is, strictly speaking, only valid for a current in which all the fluid inside the current is at rest in the moving frame: indeed Benjamin developed it specifically for a cavity in a liquid. Although the experiments on cavity flows include surface tension, Gardner & Crow (1970) and Wilkinson (1982) extended Benjamin's analysis to account for surface tension effects. They showed that surface tension slows the cavity, and the measured speeds were consistent with the theory.

The cavity flows have large density differences, and the fluids are immiscible. Early experiments with Boussinesq miscible gravity currents in a channel found current speeds that were also consistent with Benjamin's energy-conserving prediction. For a

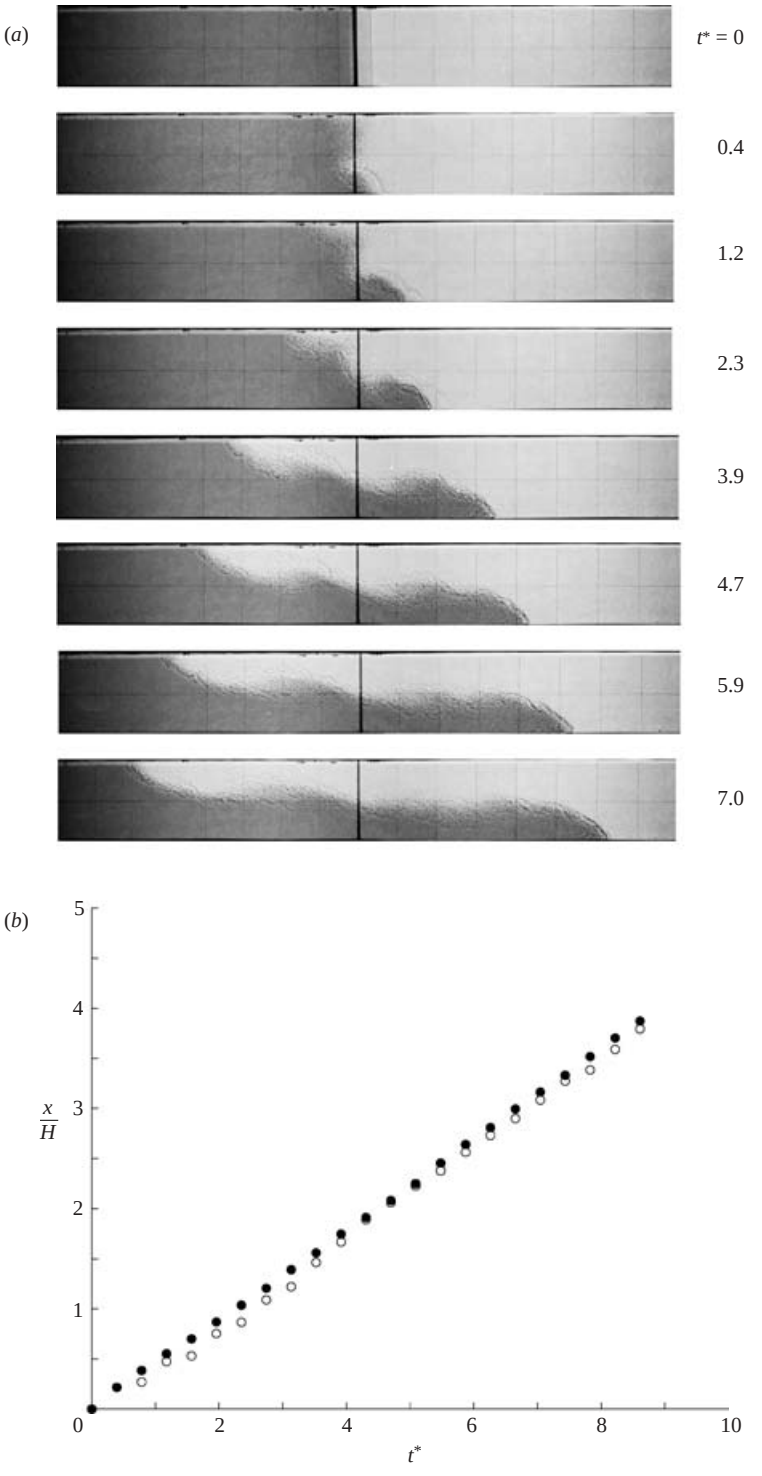

FIGURE 2. The gravity currents produced by lock-exchange in a channel. The upper and lower boundaries are rigid, and the density ratio $\gamma = 0.993$. Shadowgraph images and the positions of the two fronts are shown in (*a*) and (*b*), respectively. In (*b*) the front position x is non-dimensionalized by the channel depth H, and the dimensionless time $t^* = t\sqrt{g(1-\gamma)/H}$.

Boussinesq current with density ρ_2 in an ambient fluid of density ρ_1, the dimensionless speed is expressed as a Froude number $F_H = U/\sqrt{g'H}$, where U is the current speed, H is the channel depth and $g' = g(\rho_2 - \rho_1)/\rho_2$. Benjamin's energy-conserving theory predicts $F_H = \frac{1}{2}$. Keulegan (1958) found that the speed of the current was independent of the ratio of the channel width and depth, and measured a small increase in F_H with Reynolds number $Re = UH/\nu$, where ν is the kinematic viscosity, from $F_H = 0.42$ at $Re = 600$ to $F_H = 0.48$ at $Re = 150\,000$. Barr (1967) carried out experiments with both a free and a rigid upper surface, and used both temperature and salinity, separately, to provide the density difference. His results show that F_H increased with Reynolds number; the variation is most pronounced for Re from 200 to 1000, and there is some slight evidence that a small increase in F_H occurs for $Re \geqslant 1000$. The free-surface cases have higher values of F_H. For the rigid upper surface, values of F_H for both currents are comparable, and vary from about 0.42 at $Re = 200$, to about 0.46 for $Re \geqslant 1000$.

Unfortunately, the speed of the current is an insensitive test of the whether the current is energy conserving. As we discuss below, the difference in speeds between a current with maximum dissipation, according to Benjamin's theory, which has a depth of $h/H = 0.347$ and $F_H = 0.527$ and the energy-conserving current with $h/H = 0.5$ and $F_H = 0.50$ is very hard to resolve from experimental measurements. However, the difference in depths is large enough to be a distinguishing feature.

Recently Lowe, Linden & Rottman (2002) repeated experiments on symmetric intrusions propagating along a sharp density interface first conducted by Britter & Simpson (1981). Such an intrusion can be considered as a gravity current propagating along a free-slip boundary and reflected in that boundary. In both of these studies, the shape and speed of the intrusion was found to be well predicted by Benjamin's energy-conserving theory. Lowe *et al.* (2002) also showed that the relative flow within the intrusion was small, consistent with Benjamin's cavity theory. These experiments suggest that Benjamin's energy-conserving gravity currents are observed for Boussinesq, miscible fluids.

However, none of these previous experiments have measured the depth of the current in an objective and unambiguous way. Usually, as in the case of Lowe *et al.* (2002), the depth is inferred from visual observations. And as can be seen from figure 2, the top of the current is not clearly defined and is irregular and unsteady.

Additionally, most gravity currents, produced either by lock exchange or arising in other ways in the laboratory or in nature, do not occupy half the depth of the ambient fluid. Currents with depths significantly less than half the total depth can be easily achieved in the laboratory by using a partial-depth lock, as shown in figure 1(*b*). An example of a current produced by a lock containing dense fluid of initial depth equal to one-half the total depth is shown in figure 3. Figure 4 shows the flow when the lock depth $D = 0.83H$. In both cases a dense current travels to the right as in the full-depth release, but now the disturbance travelling to the left takes the form of a wave of rarefaction propagating on the interface. Apart from the fact that the dense current occupies significantly less than half the channel depth, qualitatively it looks much the same as the dense current shown in figure 2, except there is a more pronounced raised head near the front of the shallower current (figure 3) and the top of the current has a more pronounced slope. The second and third images in figures 3 and 4 are taken at constant time intervals, and it can be seen that the speed of the front is constant in these cases also. These currents have large Reynolds numbers so that viscous effects are small. However, there are frictional losses on the lower boundary and losses from mixing that eventually cause these currents to decelerate.

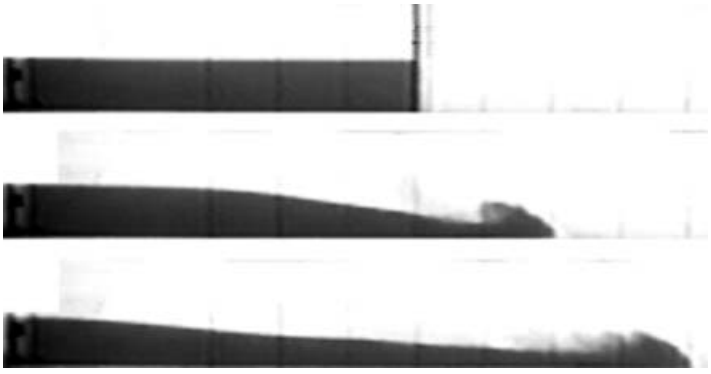

FIGURE 3. Time sequence of the flow from a partial-depth lock release. The initial depth $D = 0.5H$, and $\gamma = 0.989$.

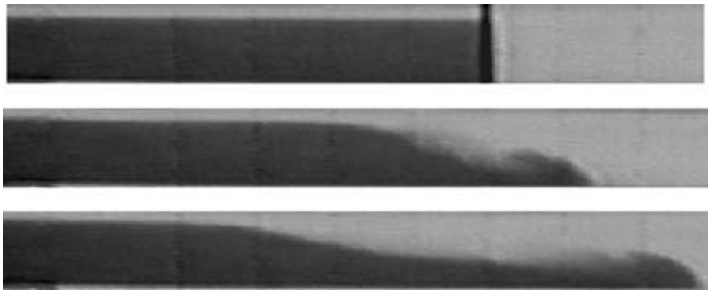

FIGURE 4. Time sequence of the flow from a partial-depth lock release. The initial depth $D = 0.83H$, and $\gamma = 0.990$.

We are concerned here with the constant-speed phase of propagation before these effects are significant.

The application of Benjamin's theory to this case implies that the energy flux entering the control volume upstream is larger than that leaving downstream of the front. He interpreted this inequality as a result of dissipation within the control volume and associated it with waves, turbulence and mixing produced by the billows on the interface behind the front of the current. Indeed, Benjamin expected that this dissipation would normally be significant and wrote that 'steady cavity flows with [depths between $0.347H$ and $0.5H$] would be difficult, if not impossible, to produce experimentally'. Probably this view came from the fact that dissipation is an essential feature of a free-surface hydraulic jump, a closely related flow. However, as we point out above, energy-conserving cavity flows were observed by Gardner & Crow (1970) and Wilkinson (1982).

Despite the intrusion observations of Britter & Simpson (1981), it is still believed that dissipation is important in the gravity currents in miscible fluids with similar densities. Klemp, Rotunno & Skamarock (1994) calculate the behaviour of lock-exchange gravity currents in a channel using both shallow-water theory and two-dimensional numerical simulations. They argue that dissipation must be included and state that 'energy-conserving gravity currents which require [half-depth] cannot be physically realized for this type of initial value problem'. From considerations of propagation along characteristics, Klemp *et al.* (1994) argue that the maximum

achievable depth is $0.347H$, which Benjamin's theory gives as the depth for the current with the maximum speed and the maximum dissipation.

There is a classical result by von Kármán (1940) for an energy-conserving current propagating in an ambient fluid of infinite depth. In that case he predicts the front speed U to be

$$F_h = \frac{U}{\sqrt{g'h}} = \frac{\sqrt{2}}{\gamma}, \tag{1.1}$$

where $g' = g(\rho_2 - \rho_1)/\rho_2 = g(1-\gamma)$ is the reduced gravity and h is the depth of the current. Benjamin suggests that since von Kármán applied Bernoulli's theorem along the interface on the top of the current to obtain this result, his argument is wrong since there is dissipation there. Benjamin then provides an alternative argument that applies Bernoulli's theorem along a streamline far above the current where the ambient fluid is at rest, and obtains the same result. This Froude number corresponds to the zero-depth, energy-conserving current found by Benjamin (1968), in the limit $h/H \to 0$ obtained as $H \to \infty$.

From experiments with Boussinesq currents ($\gamma \simeq 1$), Huppert & Simpson (1980) suggest that, in a deep ambient fluid, the numerical value of this dimensionless speed F_h is 1.19, significantly less than the theoretical value $\sqrt{2}$. They attribute this discrepancy to the dissipation in the flow. In this case the depth h of the current used in the definition of F_h is taken from visual observations and Huppert & Simpson (1980) state that they take as the value of h the depth 'just behind the head'.

The purpose of this paper is to determine the form of the gravity current produced by lock exchange. We conduct experiments on full-depth lock-exchange currents and make objective measurements of the current depth in an attempt to determine whether energy-conserving currents can be observed in the Boussinesq limit for miscible fluids. We then consider the relation of these currents to those generated by partial-depth lock exchange, where the current is significantly shallower than the half-depth of the channel.

We develop a theory for these partial-depth releases that is a generalization of Yih (1965) in which he calculates the energy-conserving flow of a symmetric, full-depth lock exchange. Yih presents results of his MS thesis (Yih 1947) in which he compares the speed from experiments with his theory which predicts the same Froude number as Benjamin's half-depth current. We show that for these partial-depth releases, energy and momentum is communicated between the two sides of the lock, and that this affects the propagation speed for shallow releases. In particular, we predict a Froude number based on the current depth $F_h = 1$ for propagation into an infinite environment.

We first describe Benjamin's (1968) theory in § 2. We examine the assumptions in his theory and show, by reference to experiments, how they apply to Boussinesq gravity currents. New experiments for Boussinesq lock releases are described in § 3. In § 4 we discuss the results of full-depth and partial-depth releases. In § 5 we develop a new energy-conserving theory for partial-depth releases. This theory, like Benjamin's, is an approximate hydraulic theory, and we compare the results with the experiments described in § 4. We discuss how the new theory connects with Benjamin's theory in § 6 by discussing wave propagation in the system. The link with shallow-water theory is explored in § 7. We consider the case of a deep ambient flow in § 8 and present new experiments in which we measure the front Froude number unambiguously. Finally, § 9 provides conclusions and comparisons with other results on gravity currents.

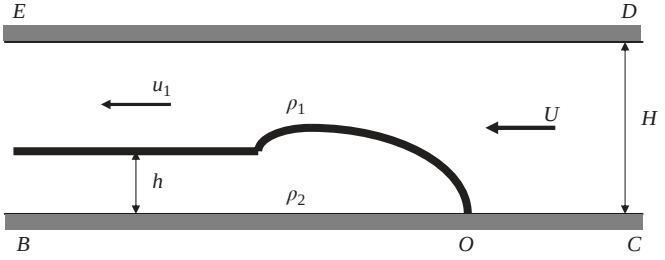

FIGURE 5. A schematic diagram of an idealized gravity current in the rest frame of the current.

2. Benjamin's theory

Benjamin (1968) derived a theory for the steady propagation of a gravity current in a rectangular channel, in which the flow may be considered as two-dimensional. He assumed that the flow far upstream and downstream of the front was hydrostatic and that within the current there was no relative flow. Hence, in a frame of reference moving with the front, the fluid in the current is at rest. In fact, as mentioned above, Benjamin (1968) developed his theory for a cavity of zero-density fluid propagating into a stationary liquid. The use of a cavity removes the need to specify the relative flow within the current. In the theory presented here we keep the two densities as ρ_1 and ρ_2, but still assume that the whole current moves as a slug without internal flow relative to the advancing front. This seems to be a good assumption as the velocity measurements in an intrusion by Lowe *et al.* (2002) show that internal velocities are typically about 10% of the current speed.

We consider a current of density ρ_2, propagating with constant velocity U into fluid of density ρ_1, and work in the rest frame of the current as shown in figure 5. We denote the depth of the current far behind the front where the interface is flat by h, and suppose that the velocity in the ambient fluid there is u_1 (assumed uniform with depth). Continuity implies that

$$U H = u_1(H - h). \tag{2.1}$$

Since there are no horizontal external forces acting on the flow, the net flux of horizontal momentum into a control volume including the front is zero. Consider the control volume consisting of two vertical planes, one downstream of the front at BE and one upstream at CD, and the top and bottom boundaries of the channel. (The reason for this seemingly strange lettering will become clear in § 5.)

Conservation of the horizontal component of the momentum flux may then be written as

$$\int_B^E p\,\mathrm{d}z + \int_B^E \rho u^2\,\mathrm{d}z = \int_C^D p\,\mathrm{d}z + \int_C^D \rho U^2\,\mathrm{d}z. \tag{2.2}$$

The pressure distributions along the two lines BE and CD may be determined since the flow is assumed to be hydrostatic. Along BE

$$p = \begin{cases} p_B - g\rho_2 z, & 0 < z < h, \\ p_B - g\rho_2 h - g\rho_1(z-h), & h < z < H, \end{cases} \tag{2.3}$$

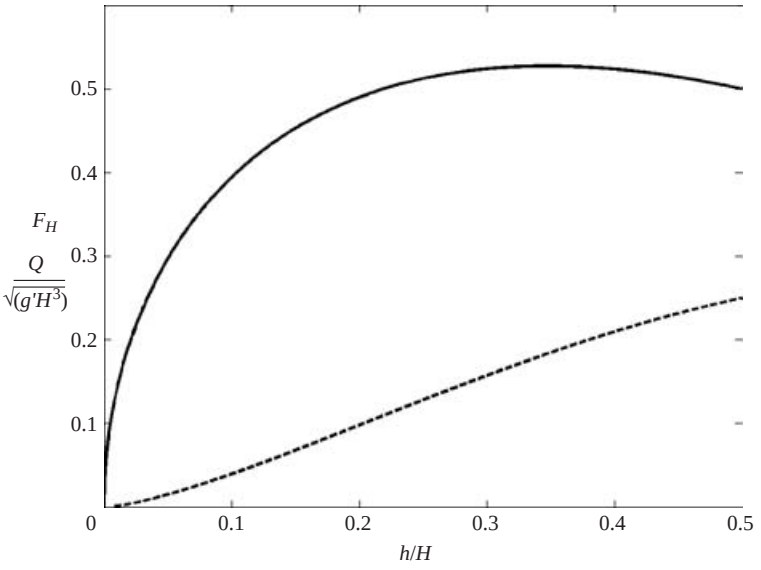

FIGURE 6. The Froude number F_H (—) and the dimensionless volume flux $Q/\sqrt{g'H^3}$ (- - - -) plotted against the dimensionless current depth h/H.

where p_B is the pressure at B. Similarly along CD

$$p = p_C - g\rho_1 z, \tag{2.4}$$

where p_C is the pressure at C.

We define the pressure at the stagnation point O to be p_O. Since, in this reference frame, the velocity within the current is zero, application of Bernoulli's equation along BO gives $p_B = p_O$, and along OC gives $p_C = p_O - \frac{1}{2}\rho_1 U^2$. Substitution of (2.3) and (2.4) into the momentum balance (2.2) and use of the continuity equation (2.1) gives

$$\frac{U^2}{gH} = \frac{(1-\gamma)}{\gamma} f(h), \tag{2.5}$$

where

$$f(h) = \frac{h(2H-h)(H-h)}{H^2(H+h)}. \tag{2.6}$$

The Froude number $F_H \equiv U/\sqrt{g(1-\gamma)H}$ and the volume flux Q are plotted as functions of h/H in figure 6. The speed of the current increases to a maximum value of $F_H = 0.527$ at $h/H = 0.347$ and then decreases again to $F_H = 0.50$ at $h/H = 0.50$. The volume flux Q is a monotonically increasing function of the current depth. Values of $h/H > 0.5$ can only be achieved by an external energy input (see figure 7) and so are not plotted.

In order to completely determine the flow it is necessary to use a further condition to specify h. As Benjamin (1968) showed, if there is no dissipation in the flow we may apply Bernoulli's equation along another streamline to determine h. The choice of either the upper boundary of the channel or the interface between the two fluids gives the same result

$$\frac{U^2}{gH} = 2\frac{(1-\gamma)}{\gamma}\frac{h(H-h)^2}{H^3}, \tag{2.7}$$

as the flow is hydrostatic far upstream. Equating the two expressions for the current speed U, gives two solutions for the current depth

$$\frac{h}{H}=0 \quad \text{or} \quad \frac{h}{H}=\frac{1}{2}. \tag{2.8}$$

The second of these solutions shows that an energy-conserving current occupies one-half the depth of the channel and travels with a non-dimensional speed

$$\frac{U^2}{gH}=\frac{1}{4}\frac{(1-\gamma)}{\gamma}. \tag{2.9}$$

For a Boussinesq current, $\gamma \approx 1$, (2.9) shows that the Froude number defined in terms of the reduced gravity and the channel depth is

$$F_H=\frac{U}{\sqrt{g(1-\gamma)H}}=\frac{U}{\sqrt{g'H}}=\frac{1}{2}. \tag{2.10}$$

Gravity currents that occupy less than half the channel depth do not conserve energy, in the sense that the energy fluxes through the vertical sections of the control volume are not equal. The energy flux $\dot{E}$ across a vertical plane is given by

$$\dot{E}=\int_0^H \left(p+\tfrac{1}{2}\rho u^2+g\rho z\right) u \,\mathrm{d}z. \tag{2.11}$$

Substituting for the vertical profiles of velocity, density and pressure gives at the upstream plane CD,

$$\dot{E}_{CD}=p_0 U H, \tag{2.12}$$

and, at the downstream plane BE,

$$\dot{E}_{BE}=p_O U H-g(\rho_2-\rho_1)UHh+\rho_1\frac{U^3H^3}{2(H-h)^2}. \tag{2.13}$$

Subtracting (2.13) from (2.12) and using (2.5) we obtain the net energy flux entering the control volume $BECD$ from upstream (i.e. from the right in figure 5) $\Delta\dot{E}\equiv\dot{E}_{CD}-\dot{E}_{BE}$. Substituting for the current speed U from (2.5), we obtain the dimensionless energy flux entering from upstream

$$\Delta\widehat{\dot{E}}=\frac{\Delta\dot{E}}{\rho_1 g'^{3/2}H^{5/2}}=\frac{h^{5/2}(H-2h)(2H-h)^{1/2}}{2H(H+h)^{3/2}(H-h)^{1/2}}. \tag{2.14}$$

The dimensionless net energy flux $\Delta\widehat{\dot{E}}$ is plotted in figure 7. The energy flux increases from zero with h, reaches a maximum when $h=0.347H$, the same depth at which the current has the maximum speed, and then decreases to zero, as expected, for the energy-conserving current $h=\frac{1}{2}H$. Over this range of h/H, $\Delta\widehat{\dot{E}}>0$, implying that energy entering the control volume upstream at CD is greater than that leaving at the downstream section BE. Benjamin (1968) interpreted this change in energy as a loss caused by some dissipative process, and calculated an equivalent head loss.

For the case of $h>\frac{1}{2}H$, the energy leaving the downstream section is greater than that entering from upstream. This is clearly impossible unless there is an alternative energy supply within the control volume.

As mentioned in §1, in an infinitely deep environment, the energy-conserving solution $h/H=0$ is non-trivial. It corresponds to the limit $H\to\infty$, keeping h finite,

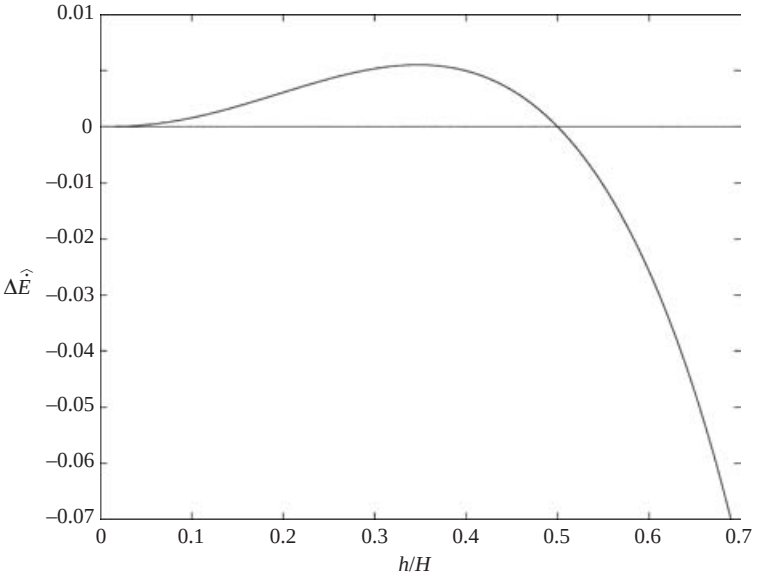

FIGURE 7. The dimensionless net energy flux $\Delta\hat{\dot{E}}$ plotted against the dimensionless current depth h/H.

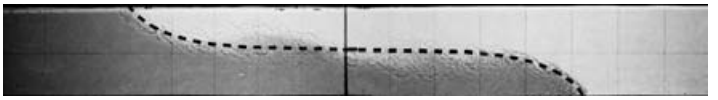

FIGURE 8. A full depth-lock release with Benjamin's (1968) potential flow solution (dashed curve) for the shape near the front superimposed on both the heavy and light currents. These local solutions are joined by a horizontal straight line.

and in that limit (2.5) gives the Froude number F_h based on the current depth as $\sqrt{2}$, the same result (1.1) as found by von Kármán (1940).

It is interesting to note that, even when the energy dissipation is a maximum, it only represents about 10% of the rate of loss of potential energy in the lock exchange. Indeed, Benjamin (1968) predicted the shape of the current for the energy-conserving case (it is a potential flow solution similar to the Stokes wave of maximum amplitude, which he calculated using a conformal transformation). His prediction is compared with a Boussinesq lock-exchange current in figure 8. Clearly the shape agrees well. Similar agreement for an intrusion was reported by Lowe *et al.* (2002).

Despite evidence of this kind, the determination of the current depth remains an open question. We address this question by the experiments described in the next section.

3. Experiments

The experiments are straightforward. As shown in figure 1(*b*), fluid of density ρ_1 is separated by a vertical barrier – the lock gate – at the mid-point of a rectangular channel of depth H from fluid of density ρ_2, with $\rho_2 > \rho_1$. The dense fluid occupied a depth $D \leqslant H$. Most of the experiments were conducted in a channel 2 m long, 0.2 m wide and was filled to a depth of $H = 0.2$ m. In most experiments the upper

surface was free, but in some cases the upper boundary was rigid and consisted of two sheets of Perspex in contact with the fluid surface, and separated by a thin gap to allow the lock to be removed. The flow was started by rapidly removing the lock gate vertically through the gap. In some experiments different sized channels were used. The dimensions of these channels are given below.

The flow was visualized either by adding dye to the dense fluid or by using a shadowgraph, created by covering the front of the tank with tracing paper and positioning a projector behind the tank. Video and still photographs were made of the flow, which were used to measure the depths and front positions of the gravity current interface. The video images were digitized with a time resolution of 1/30 s, allowing the velocity of the two fronts to be determined. Care was taken to avoid parallax errors.

The less dense fluid ρ_1 was freshwater and the denser fluid ρ_2 was a solution of sodium chloride. Densities were measured using a density meter with an accuracy of $10^{-2}\,\mathrm{kg\,m^{-3}}$.

There have been many similar experiments in the past, but most have been restricted to short locks, with lengths that are a small fraction of the total length of the tank. In almost all the present experiments the lock gate was halfway along the tank to avoid the effects of a finite-length lock, and the heavy and light currents propagated, uninfluenced by the finite length of the tank, until one of the currents got close to an endwall. At that point the experiment was terminated.

Density differences were chosen so that the currents had Reynolds numbers $Re = UH/2\nu > 1000$. It is believed (Simpson 1997, p. 152) that for these values of the Reynolds numbers viscous effects are unimportant. Flows were also restricted to Boussinesq currents with $\gamma > 0.90$. A total of 140 experiments were carried out covering a range of partial lock depths $0.11 \leqslant D/H \leqslant 1$. Vertical error bars on the figures represent two standard deviations obtained from the scatter in the measurements from repeated experiments with the same conditions. In every case this scatter is larger than any imprecision in the measurements, and probably results mainly from disturbances caused by removing the lock gate.

We have conducted some experiments specifically designed to measure the front Froude number in a deep ambient fluid. We used a deeper tank for these experiments, 0.5 m deep, 0.15 m wide and 2.37 m long. We carried out partial-depth lock-release experiments for light currents which flowed along the surface. The tank was filled to a depth of 0.485 m, and the lock gate was placed closer to one end of the tank and had a length of 0.73 m. The currents were measured during the time before the rarefaction wave reached the end of the lock, so its finite length was unimportant. The lock was filled with water and dyed with a trace of potassium permanganate, and the density of the ambient fluid was approximately 1050 kg $\mathrm{m^{-3}}$. The lock depths were approximately 55 mm, giving fractional depths $D/H = 0.11$, smaller than we were able to achieve in the original tank. The Reynolds numbers of the currents based on the lock depth, $Re = \sqrt{g'D^3}/2\nu$, were about 4500, so viscous effects were unimportant. Other experiments were run in this tank with $H = 0.20$ m, giving $D/H = 0.21$.

We also carried out experiments on full-depth lock releases that were designed to measure the depth of the current objectively. These were done in different channels and the dimensions are given in the relevant figure captions. As with the deep-ambient fluid experiments, the fluid on one side the lock was dyed with potassium permanganate. The currents were backlit and filmed at 24 frames per second with a digital video camera with a green filter over the lens. The light is absorbed by the dye and the intensity of the image is related to the dye concentration along the light path from

the back to the front of the tank. With this arrangement the reduction in intensity is exponentially related to the dye concentration. Since potassium permanganate diffuses at about the same rate as sodium chloride (in both cases diffusion is negligible for this flow), the dye concentration is a surrogate for the salt concentration and, therefore, the density. The intensity measurements then give the width-average density in the current. These measurements were analysed to determine both the front speed U and the current depth h, and subsequently the Froude number.

For the purposes of determining the local Froude number of the current the depth h of the current is not determined directly. The denominator of the Froude number (1.1) requires the product $g'h$, which is the driving pressure for the current, and is unambiguously given by the vertical integral of the density

$$\overline{g'h(x,t)} = g\int_0^H \frac{\rho(z)-\rho_1}{\rho_2}\,\mathrm{d}z. \tag{3.1}$$

Use of (3.1) removes the need to make a subjective judgement of the depth of the current, in contrast with most previous experiments.

The values $\overline{g'h(x,t)}$ were determined at each time step by plotting the summed intensity along vertical lines, located at each horizontal pixel, that span the image from the boundary to deep into the ambient fluid. The sum gives the integral of the density difference between the current and the ambient fluid, and so is equivalent to the driving pressure $\overline{g'h(x,t)}$ defined by (3.1).

In circumstances where the depth is needed, it is defined by

$$\overline{h(x,t)} = \frac{\overline{g'h(x,t)}}{g_0'}, \tag{3.2}$$

where g_0' is the initial reduced gravity in the lock. If the interface between the fluids was sharp and there had been no mixing, then $\overline{h(x,t)}$ would be the height of the interface at each horizontal location. The effect of mixing is to reduce the local g' and smear out the interface, so that if the dye is placed on the dense side of the lock, $\overline{h(x,t)}$ will be smaller than the maximum height of the dye.

4. Results

4.1. *Full-depth locks*

Figure 2 shows images and front positions for a full-depth release. In this case the speeds of the light and heavy currents are constant and nearly the same. There is a slight offset as the upward motion of the gate allows the heavy current to start first, but the slopes of the lines are indistinguishable within experimental accuracy. The flow is symmetrical about the centreline, with the leading part of each current occupying about one half of the depth. Despite some mixing the mean shape of the interface between the two counter-flowing layers is stable, and is at mid-depth at the lock gate position. The speed for both fronts in this case corresponds to $F_H = 0.48$.

Figure 9 shows the evolution of a gravity current for which quantitative measurements of the depth were made. Superimposed on this figure is the depth, shown as the red curve, defined by (3.2). The energy-conserving depth $h = \frac{1}{2}H$ and the maximum-dissipation depth $h = 0.347H$ are also shown in the figure. It is clear that the depths of both the heavy and the light currents are greater than the maximum-dissipation depth and are much closer to the energy-conserving half-depth. Possibly the light current is closer to the energy-conserving depth, but the heavy current is very close to it also. The speed of the heavy current is $F_H = 0.44$.

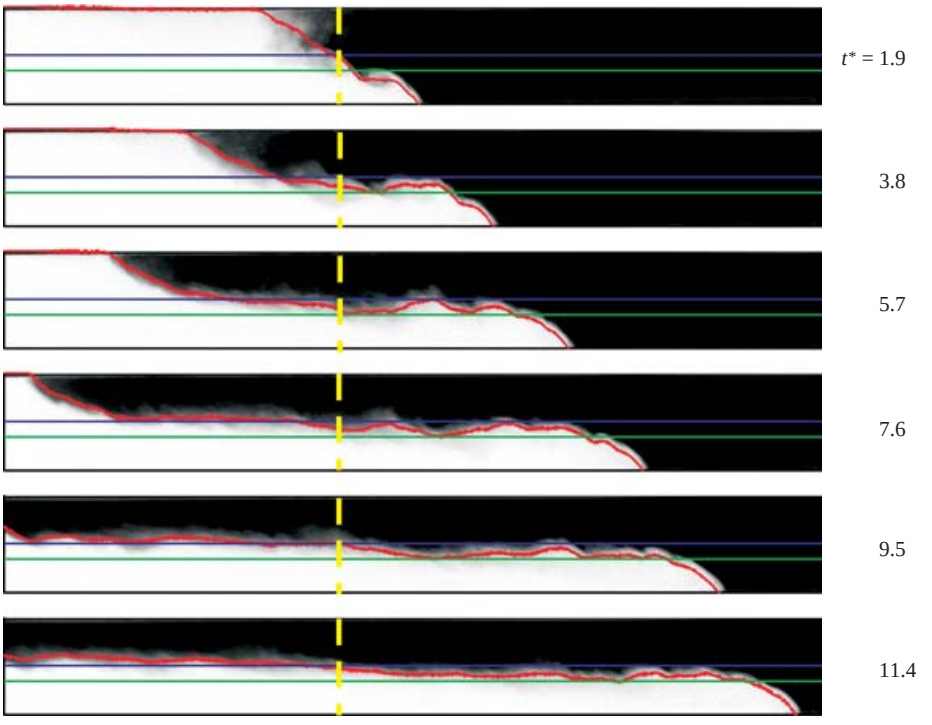

FIGURE 9. A full depth-lock release with $g' = 29.7\,\mathrm{mm\,s^{-2}}$ and $H = 0.2\,\mathrm{m}$. The red curve corresponds to the depth $\overline{h(x,t)}$ of the current, and the blue line corresponds to the energy-conserving depth $0.5H$ and the green line to the maximum-dissipation depth $0.347H$. The position of the lock is marked by the yellow dashed line and times t^* are non-dimensionalized as in figure 2. An animation of this experiment is available as a supplement to the online version of the paper.

Thus the gravity current shown in figure 9 is an example of a current that is described well by Benjamin's energy-conserving theory. Figure 10 shows another example in the same tank with almost identical parameters. The main difference in this experiment is that the lock gate was not vertical but was initially at an angle of about 40°. The slope of the gate was such that the base was to the right of the top (i.e. in the direction of the current motion). In this case the light current again seems quite close to the energy-conserving depth, but the heavy current is significantly shallower. This seems to be a result of the considerable disturbance caused by removing the gate, which was pulled out parallel to its original orientation. This disturbance is visible in the first two panels of figure 10. This causes the interface between the heavy and light currents to have a significant slope, and the depth of the current to be significantly lower than the energy-conserving current and closer to the maximum-dissipation depth. We found considerable variability in the current depths in what were essentially repeat experiments. The speeds in all cases were within 5–10% percent of the energy-conserving value $F_H = 0.5$, but the depths, especially of the heavy current varied from about $0.35H$ to $0.5H$.

The conclusion from these experiments is that the depth of the current produced from a full-depth lock release is not unique, but varies over a range depending on the initial conditions. On the other hand the range of variability is not large and, when the initial disturbances are small, the current is described to first order by Benjamin's energy-conserving theory. Given the other approximations in the theory, for example

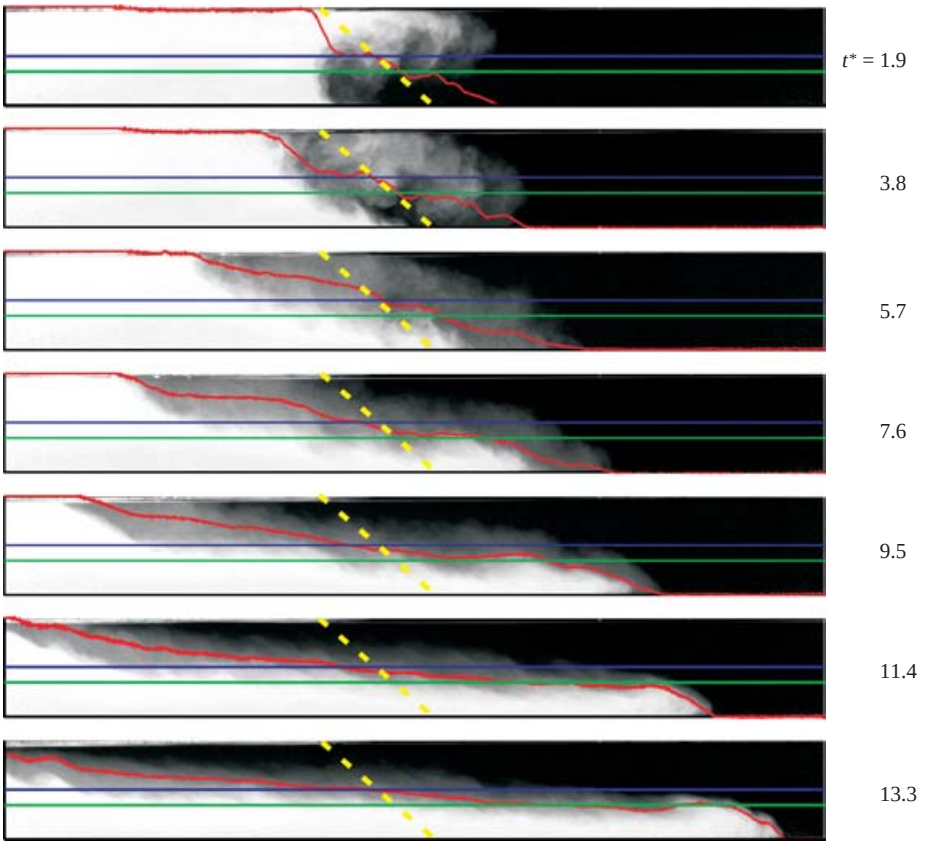

FIGURE 10. A full depth-lock release with $g' = 29.1\,\mathrm{mm\,s^{-2}}$ and $H = 0.2\,\mathrm{m}$ and the lock gate at an angle. The red curve corresponds to the depth $\overline{h(x,t)}$ of the current, and the blue line corresponds to the energy-conserving depth $0.5H$ and the green line to the maximum-dissipation depth $0.347H$. The position of the lock is marked by the yellow dashed line and times t^* are non-dimensionalized as in figure 2. An animation of this experiment is available as a supplement to the online version of the paper.

that it is assumed that there is no internal flow within the current, it seems to provide a reasonable description.

4.2. *Partial-depth locks*

However, it is clear that Benjamin's energy-conserving theory cannot be even a first-order description for very shallow currents that can easily be produced by partial-depth releases. Figures 3 and 4 show the flow for partial-depth releases with $D/H = 0.5$ and 0.83, respectively. Both show that the current has an elevated head near the front followed by a shallower flow. The interface slopes gently down from the position of the lock until it reaches the head. There is a disturbance that propagates to the left which takes the form of a rarefaction wave in figure 3 and has a more bore-like shape in figure 4. Although the data are not shown here, both the current and the rarefaction travel at constant speeds as has been observed by others in the past.

A difference between the partial-depth and full-depth releases is shown in figure 11. This figure shows a false colour representation of the buoyancy $\overline{g'h}$ on an x–t plot. The region is black before the arrival of the dense fluid, and the front is marked

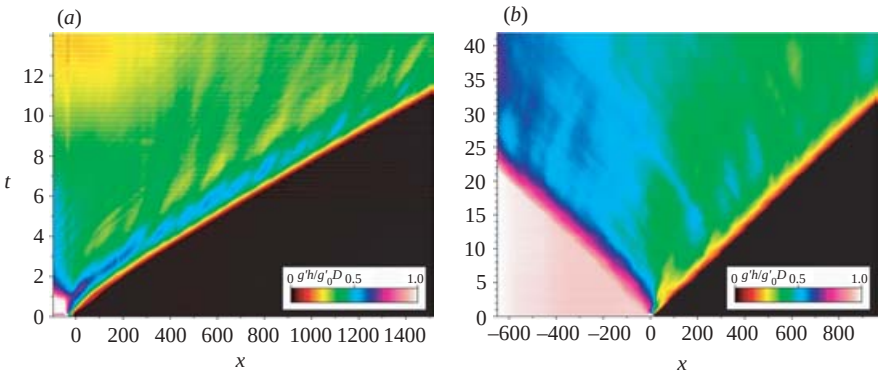

FIGURE 11. The buoyancy $\overline{g'h}$ shown by the false colour on an x–t plot for (a) a partial-release $D/H = 0.21$ and (b) a full-depth release $D/H = 1$. The intensities are normalized by the initial buoyancy $g'_0 D$ in the lock. The front position at any time is the location at the edge of the black region, and the constant front speed is shown by the straight line fit to this in (a). The blue regions behind the front are elevated values of the buoyancy indicating deep regions of the current. They travel towards the front in (a), but are almost stationary in (b).

by the transition to red. The partial-depth release is shown in figure 11(a) and the full-depth release is shown in figure 11(b). The light current (or refraction wave in (a)) is also visible and seen to travel at a constant speed. Behind the front are a series of disturbances shown by the blue streaks. These are associated with waves on the interface giving rise to perturbations to the current depth. The point of interest here is that these disturbances propagate forwards in (a), but are almost stationary in (b). This suggests that there may be communication from the rear by these waves in the case of partial-depth releases. We will discuss this issue in § 6.

Before presenting quantitative data for the partial-depth lock releases, we investigate the consequences of an energy-conserving theory for these currents.

5. Partial-depth lock releases

A full analysis of the partial-depth lock release must include a discussion of the whole system, as was first done for the full-depth release by Yih (1965). In particular, there is a possibility that energy and momentum may be transferred along the interface by internal waves, so that the properties of the current in the region of the head are modified by these inputs. We will show that energy and momentum can be transferred towards the current front for partial-depth locks less than about $0.76H$, but for deeper locks the current travels faster than long interfacial waves. Hence, for lower fractional depths Benjamin's (1968) analysis requires modification to allow for this energy transfer.

We consider the flow from a partial-depth lock as shown in figure 12. We observe that, for sufficiently large Reynolds numbers, the current and the wave of depression travel at constant speeds. We develop a hydraulic model for the unsteady flow, including both the current front and the wave of depression. We assume that the front and the wave are joined by a horizontal interface and, in the spirit of a hydraulic theory, that the flow in each layer is independent of depth. This assumed form of the flow is, of course, only an approximation to the real flow. It is chosen because it is simple enough to allow an analytical theory to be developed, and we will show

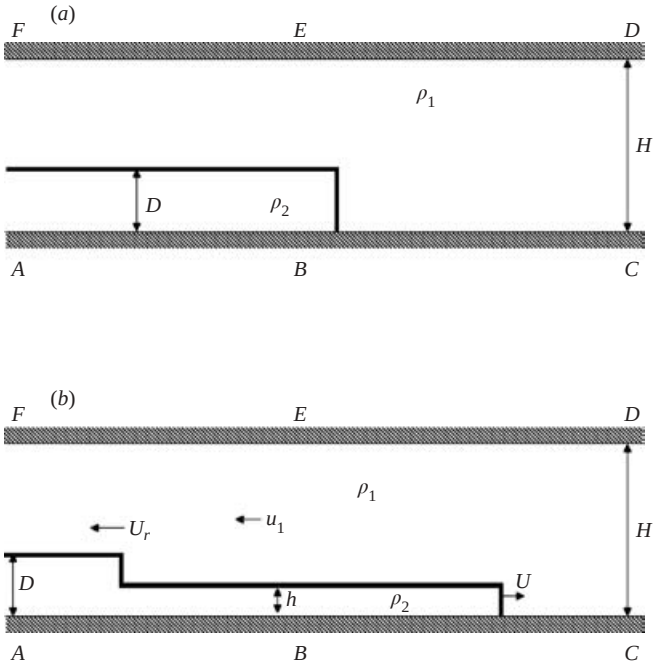

FIGURE 12. Schematic of a partial-depth lock release in a channel (*a*) before release and (*b*) after release. The symbols in are defined in the text.

that it provides a very satisfactory agreement with experiment. We will discuss the limitations of the model in § 9.

5.1. *Mass and momentum conservation*

Figure 12(*a*) illustrates the lock release schematically. Dense fluid of height D and density ρ_2 lies initially behind the lock gate. Light fluid of density ρ_1 lies on top of the dense fluid, as well as in front of the lock, so that the total height of fluid on both sides of the lock position is H. Fluid is initially at rest everywhere, and lies between two smooth, rigid horizontal boundaries. When the dense fluid is released, it forms a gravity current that moves away from the lock at a constant speed U from left to right. A disturbance is also formed, which travels in the opposite direction at constant speed U_r as shown in figure 12(*b*).

The fluid is assumed to be inviscid and immiscible and the flow is assumed to be irrotational in each layer. The shape of the interface is approximated by a horizontal middle section of height h and two advancing fronts. The two fronts are assumed to move at constant speeds and to have constant shapes in time. As in Benjamin's (1968) analysis, the exact shapes of the fronts do not matter as long they remain steady. As discussed in § 6, the backward disturbance is, in general, a rarefaction wave rather than a front of constant shape. Away from the advancing fronts the flow is assumed to be horizontal and, consequently, the vertical pressure gradient is assumed to be hydrostatic.

We now apply conservation of mass across the current and disturbance fronts, respectively. This gives

$$UH = (U + u_1)(H - h) \tag{5.1}$$

and

$$U_r D = (U + U_r)h. \tag{5.2}$$

Thus

$$u_1 = \frac{Uh}{H - h} \tag{5.3}$$

and

$$U_r = \frac{Uh}{D - h}. \tag{5.4}$$

We now consider the horizontal momentum balance inside the fixed box $ABCDEF$ shown in figure 12, which contains both the current and disturbance, so that it includes all the fluid affected by the lock release at all times. The fluid outside the box is therefore always at rest. In contrast to Benjamin's analysis we consider a mass and momentum balance over the whole box, which includes both the current and the disturbance which is responsible for the release of potential energy that drives the current.

We apply horizontal momentum conservation over $ABCDEF$. Since no fluid enters or leaves $ABCDEF$ in the laboratory frame, the only contribution to the momentum flux into the control volume comes from pressure forces acting on the sides CD and AF. Thus the rate of change of horizontal momentum $\dot{M}$ is

$$\dot{M} = \int_A^F p \, \mathrm{d}z - \int_C^D p \, \mathrm{d}z, \tag{5.5}$$

where the pressure distributions are given by hydrostatic formulae similar to (2.3) and (2.4). After integration, (5.5) yields

$$\dot{M} = \tfrac{1}{2} g(\rho_2 - \rho_1)d^2 - (p_D - p_F)H, \tag{5.6}$$

where p_D and p_F are pressures at points D and F, respectively.

The rate of increase of momentum inside the control volume $ABCDEF$ is given by

$$\dot{M} = \rho_2(U + U_r)Uh - \rho_1(U + U_r)u_1(H - h). \tag{5.7}$$

Using (5.1) and (5.4) and equating the two expressions (5.6) and (5.7), we find that the pressure difference along the upper boundary satisfies

$$(p_D - p_F)H = (\rho_2 - \rho_1)\left[U^2 \frac{Dh}{D - h} + \frac{1}{2} g D^2\right]. \tag{5.8}$$

Assuming that energy is conserved in the top layer, the time-dependent Bernoulli equation can be applied there to find the pressure difference between D and F. In this case Bernoulli's equation is

$$p_F + \rho_1 \left.\frac{\partial \phi_1}{\partial t}\right|_F = p_D + \rho_1 \left.\frac{\partial \phi_1}{\partial t}\right|_D, \tag{5.9}$$

where ϕ_1 is a velocity potential for the upper layer flow.

An approximation to the upper-layer velocity is to assume it is horizontal with x-component u given by

$$u = \begin{cases} 0 & \text{for } x < x_r, \\ -u_1 & \text{for } x_r < x < x_f, \\ 0 & \text{for } x > x_f, \end{cases} \tag{5.10}$$

where x_r and x_f are the positions along the x-axis of the disturbance front and the current front, respectively. This velocity field ignores the spatial variation of both acceleration of the flow over the head and the deceleration at the disturbance wave, assuming, instead, that both occur instantaneously.

A possible choice of ϕ_1, which satisfies (5.10) and is continuous for all x, is given by

$$\phi_1 = \begin{cases} 0 & \text{for } x < x_r, \\ -u_1(x - x_r) & \text{for } x_r < x < x_f, \\ -u_1(x_f - x_r) & \text{for } x > x_f. \end{cases} \tag{5.11}$$

Substituting this potential function into (5.9), we obtain†

$$p_D - p_F = \rho_1 u_1(\dot{x}_f - \dot{x}_r), \tag{5.12}$$

and so

$$p_D - p_F = \rho_1 u_1(U + U_r). \tag{5.13}$$

Using the continuity equations (5.1) and (5.4) in (5.13), and substituting the result into (5.8), after some algebra one finds an expression for the speed of the current:

$$\frac{U^2}{gH} = \frac{(\rho_2 - \rho_1)D(D-h)(H-h)}{2hH(\rho_2(H-h) + \rho_1 h)}. \tag{5.14}$$

As in Benjamin's analysis, conservation of mass and momentum does not close the problem and the speed of the current depends on its depth h. Indeed, to derive (5.14) it has been necessary to assume that there is no dissipation in the upper layer, so that Bernoulli's equation may be applied along the upper boundary. It is also clear that the current speed given in (5.14) does not, in general, reduce to the Benjamin limit (2.5) and (2.6) when $D = H$. We will discuss the reasons for this discrepancy later.

5.2. *Energy conservation*

As in Benjamin's analysis we need another condition to determine the flow completely, and we assume that the flow is energy conserving. In this case, however, we conserve energy in the whole control volume *ABCDEF*, since there are no energy fluxes in and out of its boundaries.

The rate of increase of energy $\dot{E}_G$ consists of the kinetic energy of the current and the disturbance and the increase of potential energy associated with the propagation of dense fluid to the right of *BE*, the initial lock location. Using the assumed velocity field, this rate of energy gain is

$$\dot{E}_G = \tfrac{1}{2}\rho_2 U^2(U + U_r)h + \tfrac{1}{2}\rho_1 {u_1}^2(U + U_r)(H - h) + \tfrac{1}{2}g(\rho_2 - \rho_1)Uh^2. \tag{5.15}$$

This energy is supplied by the loss of potential energy $\dot{E}_L$ as a result of the lowering of the interface to the left of the lock position *BE* at a rate

$$\dot{E}_L = \tfrac{1}{2}g(\rho_2 - \rho_1)U_r(D^2 - h^2). \tag{5.16}$$

Assuming that energy is conserved inside *ABCDEF*, we equate (5.15) and (5.16) and obtain a further relation for the current speed:

$$\frac{U^2}{gH} = \frac{(\rho_2 - \rho_1)(D-h)(H-h)}{H(\rho_2(H-h) + \rho_1 h)}. \tag{5.17}$$

† Introducing a non-hydrostatic steady contribution to ϕ_1 in the neighbourhood of the fronts will not change this result, since it does not affect (5.9).

The additional constraint of global energy conservation gives a unique value for the depth h of the current. Comparing (5.14) and (5.17) we find that the only non-trivial case is

$$h = \frac{D}{2}. \tag{5.18}$$

Thus an energy-conserving gravity current produced by a partial-depth lock release has a depth that is half the initial lock depth before release. This result is consistent with Benjamin's result (2.8) for a full-depth release $D = H$. From (5.18), the speed of the current is given by

$$\frac{U^2}{gH} = \frac{(\rho_2 - \rho_1)D(2H - D)}{2H(\rho_2(2H - d) + \rho_1 D)}, \tag{5.19}$$

and the speed of the backward disturbance is equal to the current front speed

$$U_r = U. \tag{5.20}$$

Consequently, application of mass, momentum and energy conservation yield a unique gravity current with properties determined by the initial densities and depths on the two sides of the lock. In general, the current does not occupy the half-depth of the channel, and does so only in the case of a full-depth lock release.

The above energy-conserving solution was derived without using the Boussinesq approximation. It is, therefore, theoretically valid for any pair of densities ρ_1 and ρ_2. We expect the above model to break down for non-Boussinesq fluids however. The model assumes that the current and disturbance sides can be matched by a flat interface in the middle section, where velocities are horizontal and conditions are uniform. Although laboratory experiments show that this assumption is approximately valid for Boussinesq flows and cavity flows, experiments by Keller & Chyou (1991) and Rottman & Linden (2001) show that this assumption is likely to be invalid for non-Boussinesq dense gravity currents. A discussion of the non-Boussinesq lock-exchange problem is given in Lowe, Rottman & Linden (2004) and Birman, Martin & Meiburg (2004).

Restricting attention to Boussinesq currents, $\gamma \approx 1$, (5.19) reduces to

$$F_H = \frac{U}{\sqrt{g(1-\gamma)H}} = \frac{1}{2}\sqrt{\frac{D}{H}\left(2 - \frac{D}{H}\right)}. \tag{5.21}$$

In the limit of a full-depth lock $D = H$, (5.21) reduces to the Benjamin result $F_H = \frac{1}{2}$, so that both theories give the same result for that case. However, as has already been pointed out, for partial-depth locks the results of the present theory differ significantly from Benjamin's result.

As noted above, Yih (1965) applied energy conservation globally, similar to the analysis in the present section, to derive an expression for the speeds of the two counter-flowing gravity currents in a Boussinesq, full-depth lock release. The present theory also agrees with his result in the limit $D = H$.

5.3. *Comparison with experiments*

Speeds are given here in terms of the Froude number

$$F_D = \frac{U}{\sqrt{g'D}}, \tag{5.22}$$

based on the lock depth D. The depth of the current h, which, in the present analysis is the depth where the interface is flat behind the front, is measured at the position of

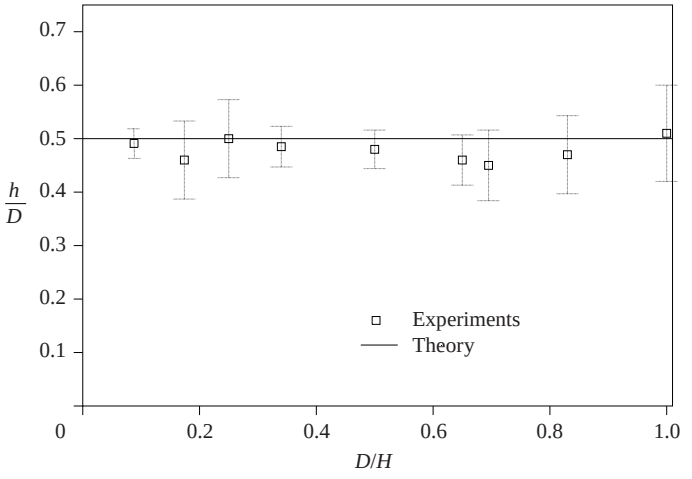

FIGURE 13. Comparison of measurements with the theoretical prediction (solid line) of the depth of the gravity current for partial-depth lock releases. Equation (5.18) predicts that $h/D = 1/2$ for all lock depths. Vertical error bars in this and the later figures represent two standard deviations in the scatter in the data from repeated experiments.

the lock. Since there is almost no mixing at this location the depth can be determined accurately. As can be seen from figures 3 and 4 the interface slopes down slightly from this depth near the head. This slope is associated with the transfer of energy and momentum from the disturbance side to the current, and will be discussed in § 6.

Figures 13 and 14 show the results for the current depths and Froude numbers as functions of the fractional depth of the lock D/H. The theoretical values given by (5.18) and (5.21) are shown as the solid lines on the figures, and the agreement is very good. The depth h is, generally, slightly lower than the predicted value (see also the Appendix), but the discrepancy is always within the scatter of the measurements. For full-depth releases $D/H = 1$, the mean depth is clearly larger than $0.347H$, as discussed in § 4.1. The observed velocities are also very close to the values predicted by the present theory over the whole range of D/H. The currents are slightly slower than predicted, but the discrepancy is at most about 10% and is usually much less, and is due mainly to bottom drag. This agreement is much better than can be obtained using Benjamin's theory (Shin 2002), except when $D/H \approx 1$, when the two theories give the same speed. Thus it seems that the present energy-conserving theory provides an acceptable description of the experiments for the full range of lock depths tested.

6. Resolution of the energy paradox

As discussed in § 5, Benjamin's theory only agrees with experiments for near half-depth, energy-conserving currents generated by full-depth lock releases. On the other hand, the new model agrees well with experiments for all initial fractional depths. This difference suggests that current and disturbance sides interact in a lock release, so that Benjamin's analysis is not valid in general. The amount of interaction is difficult to quantify. Benjamin's (1968) model assumes that no energy and momentum can be transferred between disturbance and current sides and does not consider the possibility of long waves entering the system. Obviously waves can propagate along the interface between the denser and lighter fluid and these waves can carry energy

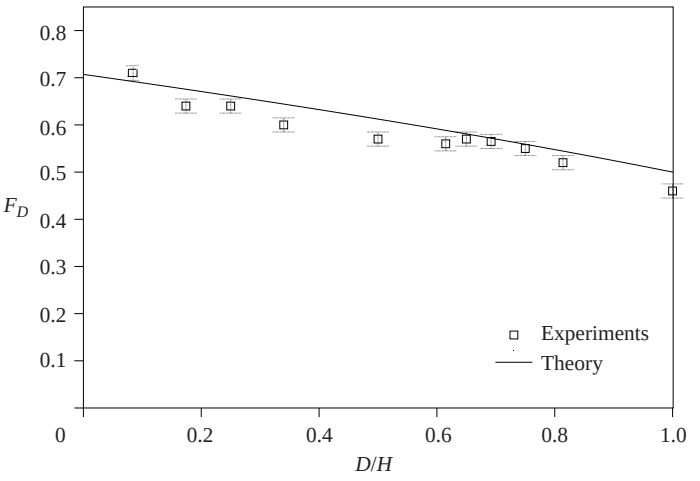

FIGURE 14. Gravity current speeds, expressed non-dimensionally as Froude numbers based on the depth of the lock D, compared with the theoretical values (5.21) shown as the solid curve.

and momentum – see figure 11. This transfer modifies the energy and momentum balance on the current side, so that Benjamin's analysis is, in general, not appropriate.

As explained in § 2, dissipation must be introduced in Benjamin's analysis to enable a steady current to occupy less than half the channel depth. This dissipation is no longer needed in the new model, where disturbance and current sides are both considered in the energy balance. The disturbance continually releases potential energy as it advances through the fluid. This introduces additional terms in the energy equation that balance the energy terms on the current side, allowing energy to be conserved overall. Benjamin's analysis which considers the energy fluxes into a control volume surrounding only the current shows, correctly, that the net energy flux is non-zero when the current is not a half-depth current. Benjamin concludes that the difference in energy fluxes is dissipated. We argue that it results from transfers from the disturbance side which are excluded from Benjamin's analysis.

The speed of long waves on the interface can be obtained from shallow-water theory. As shown in Baines (1995) the speed of long waves $c_\pm$ is given by

$$\frac{c_\pm}{U} = \frac{H-2h}{H-h} \pm \sqrt{\frac{g(1-\gamma)}{U^2}\frac{h(H-h)}{H} - \frac{h}{H-h}}, \tag{6.1}$$

where c_+ and c_- refer to right- and left-propagating waves, respectively. Substituting for the current speed from (5.21) we have, in the Boussinesq limit,

$$\frac{c_\pm}{U} = \frac{H-2h}{H-h} \pm \sqrt{\frac{H-2h}{H-h}}. \tag{6.2}$$

In terms of the initial lock depth D, (6.2) is

$$\frac{c_\pm}{U} = \frac{2(H-D)}{2H-D} \pm \sqrt{\frac{2(H-D)}{2H-D}}. \tag{6.3}$$

These wave speeds are plotted against the fractional depth of the release in figure 15. The right-travelling wave c_+ has speed U, when $2(H-D)/(2H-D) = \frac{1}{2}(3-\sqrt{5}) = 0.382$, which occurs when $D = 0.76H$. For shallower locks the current

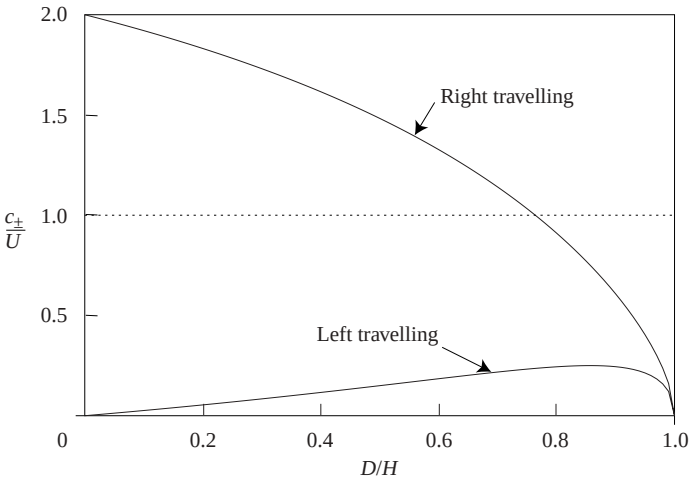

FIGURE 15. The speeds $c_\pm/U$ of waves on the top of the current plotted against the fractional depth D/H of the release. Waves travelling to the left are always slower than the current, while waves travelling to the right are faster for $D/H < 0.76$.

travels slower than long waves and energy and momentum may be transferred from the disturbance side to the current side. Thus Benjamin's theory cannot apply for partial-depth releases with $D < 0.76H$, and the theory presented here applies. For locks with $D > 0.76H$, the current travels faster than all long waves and Benjamin's theory should be approximately correct. Comparison of (2.5) and (5.21), taking the current depth in the former to be close to half the lock depth, gives very close numerical agreement. For example taking a lock release of $D = 0.8H$, the two theories give values of the Froude number F_D of the current as 0.49 and 0.52, respectively.

This dependence on the initial lock depth is illustrated in figure 15, which shows that c_+/U increases with decreasing D/H and reaches a limit of 2 in the limit of very shallow locks $D \to 0$. This ability of the long interfacial waves to travel faster than the current as the current becomes shallower results from two effects. First, the current itself travels more slowly as the depth increases and, second, the wave speed depends on the depths of both layers, and so waves can propagate faster on the deeper upper layer in this limit.

Long waves travel in general much faster towards the right than towards the left: about ten times faster for $D = 0.12H$ and about 35 times faster for $D = 0.05H$. The asymmetry occurs because the velocity in the upper layer decreases as the current becomes shallower. Assuming that the energy flux is proportional to the group velocity, long waves carry more energy towards the right than towards the left at lower fractional depths. Interaction between the disturbance and current sides is, therefore, expected to be strongest at lower fractional depths.

These theoretical results are in agreement with the observations in figure 11, which show waves travelling faster than the front for a shallow current, but slower for a deeper current.

The structure of the disturbance depends on whether it travels faster than infinitesimal long waves on the undisturbed interface. The speed c of the latter is given by standard theory (see e.g. Turner 1973, § 2.1.7)

$$\frac{c^2}{g(1-\gamma)H} = \frac{D(H-D)}{H^2}. \tag{6.4}$$

Comparison with (5.20) shows that the disturbance will be a bore provided

$$2H - D > 4(H - D), \tag{6.5}$$

and this occurs when $D > \frac{2}{3}H$. For shallower depth releases the disturbance will be a rarefaction wave. This behaviour is in agreement with our observations shown in figures 2, 3 and 4, and the observations of Rottman & Simpson (1983).

7. Two-layer shallow-water theory

The hydraulic theory presented in § 5 assumes that the flow is hydrostatic and that regions of the flow exist where the interface is flat. It is also assumed that each layer moves like a plug, so that there is no relative flow near each front. These assumptions are necessary to obtain an analytical solution. An alternative to these approximations can be obtained by noting that, apart from the initial stages immediately after the removal of the lock gate and near the front of the current, the vertical scales of the flow are much smaller than the horizontal scales. Consequently, in the later stages the flow, in regions away from the front of the current, may be described by shallow-water theory. This theory expresses conservation of mass and momentum (but not necessarily energy) for a flow in which the velocity is assumed to be independent of depth. The closure condition in this theory is obtained from specifying the Froude number of the front, as first proposed by Abbott (1961).

This methodology was first exploited for a two-layer flow by Rottman & Simpson (1983) who solved the initial value problem corresponding to the lock release shown in figure 1(*b*). Details of the calculation are not given here, but as Rottman & Simpson (1983) show, shallow-water theory reduces to solving ordinary differential equations for the speeds and the depths of both layers. For the Boussinesq case, these equations are (see Rottman & Simpson 1983)

$$h\frac{\mathrm{d}U}{\mathrm{d}h} - (1-2a)U + \lambda_{\pm} = 0, \tag{7.1}$$

along characteristics

$$\frac{\mathrm{d}x}{\mathrm{d}t} = \lambda_{\pm}, \tag{7.2}$$

where

$$\lambda_{\pm} = U(1-a) \pm \sqrt{U^2a^2 + g'h(1-b)} \tag{7.3}$$

and, consistent with the notation used by Rottman & Simpson (1983),

$$a = \frac{h}{H-h}, \qquad b = \frac{h}{H} + \frac{U^2}{g'H}\frac{H^2}{(H-h)^2}. \tag{7.4}$$

The initial conditions are that the fluid is everywhere at rest, and that the initial depth of the dense fluid is

$$h(x, t=0) = \begin{cases} D & \text{for } x < 0, \\ 0 & \text{for } x > 0. \end{cases} \tag{7.5}$$

Two further conditions are needed. If the backward disturbance from the lock is a rarefaction wave, the velocity of the dense fluid is zero at the leading edge of the disturbance, so that

$$U = 0, \quad \text{when} \quad h = D. \tag{7.6}$$

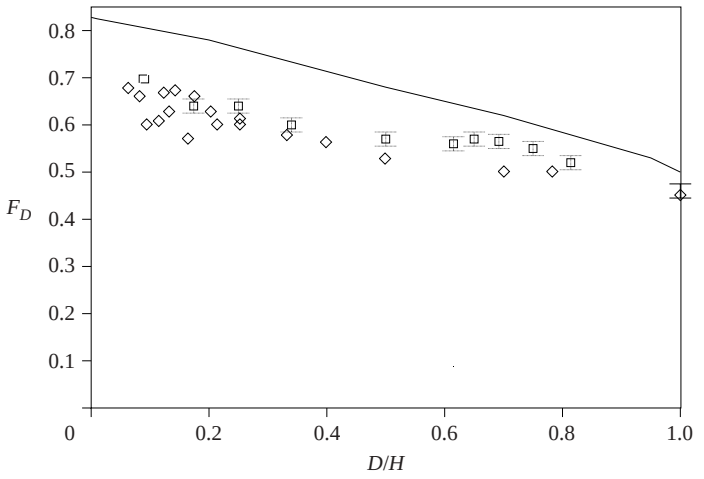

FIGURE 16. Gravity current speeds, expressed non-dimensionally as Froude numbers based on the depth of the lock D, compared with shallow-water theory (solid curve) based on Benjamin's front condition, for the full range of lock depths. The data shown here include the present experiments (□) and those by Rottman & Simpson (1983) (◇).

As mentioned above, the final condition is set by imposing the front speed. Rottman & Simpson (1983) used a condition

$$\frac{{U_f}^2}{g'h_f} = \beta^2 \frac{(H-h_f)(2H-h_f)}{2H(H+h_f)}, \tag{7.7}$$

where U_f and h_f are current speed and depth at the front, and β is a dimensionless constant. This front Froude number reduces to Benjamin's (1968) Froude number equation (2.6) when $\beta^2 = 2$.

Figure 16 shows a comparison of this theory with measurements of the front speed from the present experiments and those of Rottman & Simpson (1983). Because of the difficulty in determining the front depth h_f in experiments, we have presented the results in terms of the Froude number F_D based on the initial lock depth D and defined in (5.22). The two sets of experiments are consistent, although Rottman & Simpson (1983) used short locks so that the rarefaction wave reached the endwall of the tank and then reflected back towards the front. As Rottman & Simpson (1983) show, the speed of the front is constant and independent of the reflected disturbance, which, for a full-depth release is a two-layer bore, until the reflected disturbance catches the front. Hence the agreement between the experiments is expected. The theoretical curve with $\beta^2 = 2$ overestimates the speeds by about 20%. Rottman & Simpson (1983) arbitrarily reduced the constant $\beta^2 = 1$, and then got good agreement with their experiments, but there is no theoretical justification for this value.

The theory given in § 5 provides an alternative front condition. From (5.18) and (5.19)

$$\frac{{U_f}^2}{g'h_f} = 1 - h_f/H. \tag{7.8}$$

In the present theory the current and the disturbance sides are assumed to be matched by uniform conditions in the middle section. As shown in § 6 the disturbance is a rarefaction wave for shallow lock releases $D/H < 0.67$. In this case the disturbance

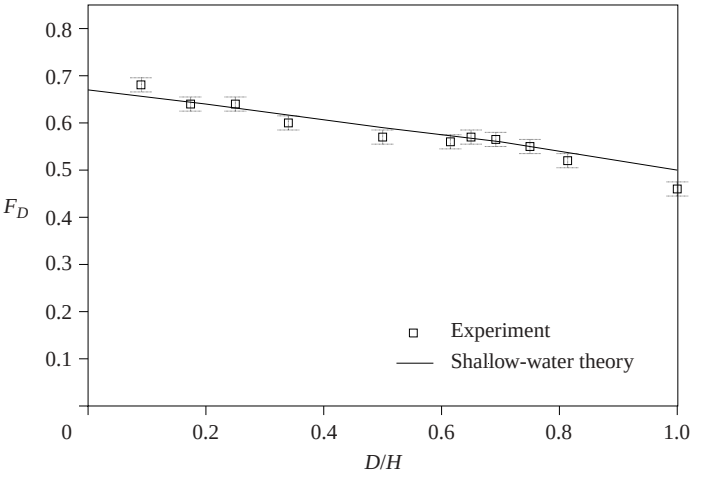

FIGURE 17. Gravity current speeds, expressed non-dimensionally as Froude numbers based on the depth of the lock D, compared with shallow-water theory (solid curve) using a front condition based on the present theory.

condition is given by (7.6). For deeper lock releases $D/H > 0.67$ a bore forms and the boundary condition is replaced by (5.20). The characteristic equation (7.2) is integrated forward in the direction of decreasing h until the front condition (7.8) is satisfied.

Figure 17 shows the front speed calculated with this new front condition and the comparison with the present experiments. In this case there is no adjustable constant in the front condition (7.8) and the agreement is very good. For shallower lock releases the agreement is significantly better than the calculations based on Benjamin's theory (figure 16), although the two calculations converge for full-depth releases as expected. Comparison with figure 14 shows that shallow-water theory gives predictions comparable to, but slightly slower than, the energy-conserving theory. The numerical differences in the predicted Froude numbers F_D are within 5%.

The agreement between the energy-conserving theory, shallow-water theory and the experiments is encouraging. Both theories conserve mass and momentum. The energy-conserving theory also conserves energy and assumes that the flow is uniform in each layer and that the interface between the two fronts is flat. Shallow-water theory does not make these assumptions and allows for spatial and temporal variations in the current speed and interface height. It, however, is not valid until some time after the release, and is not valid at the gravity current front where the flow is non-hydrostatic. It seems, though, that these various approximations are not particularly important to the description of the bulk propagation of the currents.

8. Gravity currents in a deep ambient fluid

In many geophysical and industrial flows the gravity current propagates in an ambient fluid of effectively infinite depth. As discussed in § 1 this case was considered by both von Kármán (1940) and Benjamin (1968). Taking the limit of large ambient depth $h/H \to 0$ in either (2.6) or (2.7) gives (1.1). In the limit of infinite ambient depth this gives $F_h = \sqrt{2}$. On the other hand, in this deep ambient fluid limit $h/H \to 0$, the present theory (5.21) with $h = \frac{1}{2}D$, which accounts for energy transfers between the

two sides of the lock, predicts

$$F_h = \frac{U}{g'h} = 1. \tag{8.1}$$

As also discussed in § 1, Huppert & Simpson (1980) suggest, on the basis of their own and a compilation of other experiments, that the observed Froude number $F_h = 1.19$, smaller than the value $\sqrt{2}$ predicted by von Kármán (1940) and Benjamin (1968). In fact, Huppert & Simpson (1980) suggest the empirical relation

$$F_h = \begin{cases} 1.19 & \text{for } 0 < h/H < 0.075, \\ (h/H)^{-1/3} & \text{for } h/H > 0.075. \end{cases} \tag{8.2}$$

The deep ambient fluid limit of 1.19 of these experimental values lies inconveniently between the classical prediction of $\sqrt{2}$ and the new limit of $F_h = 1$. A possible explanation for this discrepancy is in the value of the current depth h used in determining F_h. Huppert & Simpson (1980) state that they use 'the depth of the current just behind the head'. As can be seen from our experiments (figures 3 and 4) this depth is difficult to define unambiguously due to local mixing. The deep ambient fluid limit reported by Huppert & Simpson (1980) would be consistent with our theory if they used a measured depth $h_m = 0.71h$. We noted in § 4 that the depth just behind the head is less than that further back, and this smaller value may account for the difference.

An example of the flow structure for a surface current for the case $D/H = 0.11$ is shown in figure 18. The current has a deep head with billows and mixing at the rear. Immediately at the rear of the head the current is shallower than both the head and also the current further behind. The mixing region is confined to within one or two head heights of the front, after which the edge of the current is stable and there is no appreciable mixing. These images of the current confirm the accepted view as described, for example, by Simpson (1997). The depth is shallowest in and just behind this breaking region, and then slopes gently to a constant-depth region. This extended field of view shows more clearly than the images taken in the smaller tank that the assumption of a constant current depth is reasonable. The larger slopes seen in figures 3 and 4 are a result of the short length of the current. The present experiment shows that the slope is less significant as the current propagates further from the lock.

From these images we create a plot of the average intensities at each horizontal pixel and for each time image, and plot $\overline{g'h}$, defined by (3.2), as a function of horizontal position at each time. An example of such an x–t intensity plot for a surface current is shown in figure 19. The intensities are given by the false colour image. The motion of the front is shown by the edge of the intensities, and since this edge is straight we see that the current travels at a constant speed. The slight periodic deviations from the straight edge are a result of small-amplitude surface waves that are generated when the gate is removed. These are unavoidable for a surface current, but they can be removed from the data to get an accurate measure of the front speed. The advantage of the surface current is that the boundary is a closer approximation to the stress-free boundary assumed by the theory and it is exactly horizontal, so that the current speed is not biased by a mean boundary slope. These data are recorded for each experiment and the speed U of the front determined by a least-squares fit to the slope of the intensity edge.

From figure 19 we see that $\overline{g'h}$ is maximum just behind the front. This maximum is associated with the raised head near the front. Behind this there are regions where

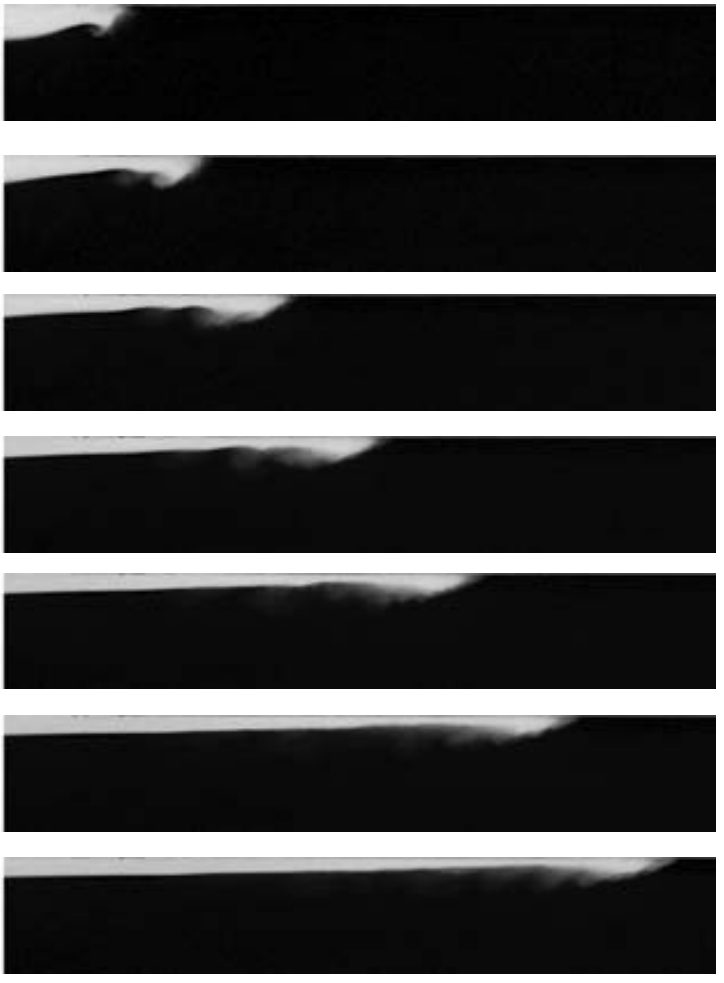

FIGURE 18. A surface gravity current. The images are taken at 1 s intervals and the field of view is 890 mm by 148 mm. The initial depth of fluid in the lock is $D = 55$ mm, and the tank depth $H = 485$ mm, so that $D/H = 0.11$. The predicted value of the Froude number F_h is 0.97, and the measured value is 1.02 ± 0.11. An animation of this experiment is available as a supplement to the online version of the paper.

the values of $\overline{g'h}$ are lower than either the head or the region behind. These occur where there are billows and the current is shallower. The flow is unsteady in this region, indicative of mixing. Further to the rear we see that the values of $\overline{g'h}$ become constant. Numerically this constant value is very close to one-half the initial value $\overline{g'h}$ in the lock, as predicted.

From these data we calculate the Froude number $F_h = U/\sqrt{\overline{g'h}}$. For comparison with the energy-conserving theory we use the value of $\overline{g'h}$ at the original position if the lock, although from figure 19 it is clear that we could use any position behind the head where the interface is flat. The predicted values from our theory give an average value of $F_h = 1.02 \pm 0.11$, while the theoretical value is $F_h = 0.97$. Thus the experiments give Froude numbers 5% larger than that predicted by the present theory. The measured values are much smaller than those cited by Huppert & Simpson (1980)

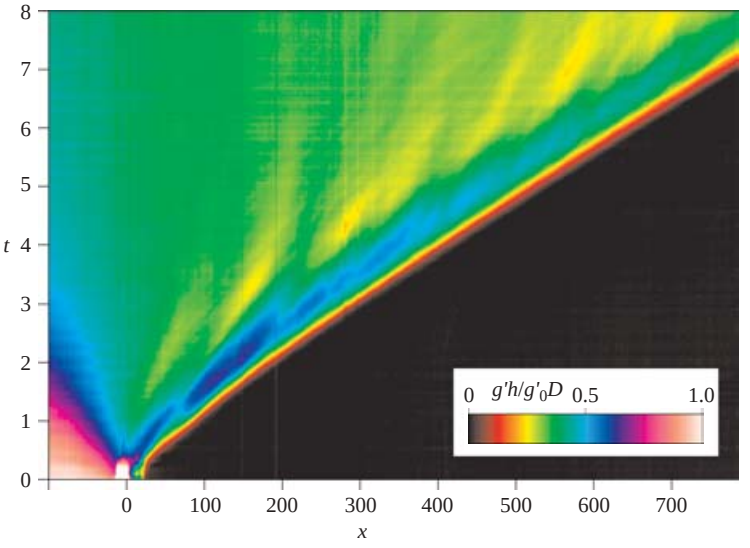

FIGURE 19. The buoyancy $\overline{g'h} = g\int_0^H(\rho(z)-\rho_1)/\rho_2\,\mathrm{d}z$ in the current shown in figure 18 in the x–t plane. The field of view is 890 mm by 8.33 s. The intensities are normalized by the initial buoyancy g'_0D in the lock. The straight front shows that the current speed is constant. The higher intensities there correspond to the elevated head, and the wave-like features correspond to the billows. The buoyancy is observed to be constant for a significant, and growing, region from the lock forwards. The lock gate is at $x = 0$.

because of the definition of $\overline{g'h}$ used. As can be seen from figure 18 using a value of h determined close behind the head will lead to a significantly larger Froude number.

It is disappointing that out experiments give values that exceed the theoretical value, as we expected friction to reduce the speed slightly from the energy-conserving theory. However, it turned out to be difficult to get a more precise value from the measurements, and the theory falls within the scatter of the data. It is possible to observe slight variations in the current speed, which depend on precisely how the front position is determined, that also produce uncertainties of a few percent in the Froude number.

We conclude that these data show that the observed front Froude number is much closer to the present theory than the classical value of $\sqrt{2}$. Analysis of previous experiments, that suggested a larger Froude number, did not determine the equivalent depth of the current as we have done through (3.1). The reason why previous experiments have recorded a larger Froude number is probably because the depth was chosen closer to the head where, as figure 19 shows, the current is shallowest.

9. Conclusions

This paper has addressed the following question. Given that Benjamin's theory for energy-conserving gravity currents predicts that the current will occupy half the depth of a channel, how do we account for observations of currents that have small fractional depths? Benjamin (1968) argued that dissipation is important in the latter cases, but since the only difference between the flows is a removal of an upper boundary to large distances it is hard to see why. Benjamin apparently believed that

all gravity currents are dissipative, but laboratory evidence (Gardner & Crow 1970; Wilkinson 1982) clearly shows non-dissipative cavity flows.

Our analysis, like that of Benjamin, uses a hydraulic approach. This has strengths and weaknesses. The strength is that if the flow is broadly hydrostatic, even if regions of the flow are distinctly non-hydrostatic, then mass, momentum and energy balances can be applied over suitable control volumes. We have done this over a control volume that includes both sides of a lock release. Benjamin only considered one side and ignored the possibility of communication between the two. Since the gravity current is driven by the release of potential energy from the disturbance, this is a significant omission. Both von Kármán (1940) and Benjamin (1968) ignore the possibility that energy may enter the control volume along the interface behind the current. We have shown that waves travel faster than the front when the current is shallow. They transport energy and momentum towards the front and must be included in the relevant budgets.

As can be seen from figures 3, 4 and 18, the flows are more complicated than the approximate model and the hydraulic approach assumed here. An approach that may be more accurate is to use two-layer shallow-water theory for these flows, as first done by Rottman & Simpson (1983). However, shallow-water theory cannot deal with the gravity current front and so a front condition must be imposed. If the front speed given by our hydraulic model (5.19) is used then the gravity current speeds can be predicted. The results are shown in figure 17, and we see that good agreement is found.

Both Benjamin (1968) and Klemp *et al.* (1994) argue that currents with fractional depths $h/H > 0.347$ cannot be realized in practice, since the current travels faster than long interfacial waves. Klemp *et al.* (1994) state that 'limitations on the fastest-moving disturbances preclude the possibility of reaching a supercritical state at the front'. They support their argument by referring to the maximum fractional depth of about 0.3 found by Simpson & Britter (1979) who measured the depth of unmixed fluid immediately behind the head of the current. This choice may not be appropriate for comparison with Benjamin's theory or the present theory, since conditions must become uniform to apply Bernoulli's theorem. On the other hand, support for the limit on the depth comes from the two-dimensional numerical simulations of a full-depth release of Härtel, Meiburg & Neckar (2000). They find that depth of the current, based on a vertical integral of the density (see their figure 14) is considerably less then the energy-conserving value and is closer to the maximum-dissipation value of 0.35. On the other hand, they also show that the instantaneous front shape (see their figure 13) is in close agreement with the theoretical shape determined by Benjamin (1968). The numerical simulations of Klemp *et al.* (1994) also support this limit (see their figure 12*b*) since the depth based on the buoyancy integral is always less than the $0.347H$ limit.

However, our measurements unambiguously show that deeper Boussinesq currents can be produced by lock exchange. The restriction of $h/H < 0.347$ comes from a consideration of the speed of characteristics, as though this is a classical piston problem. However, since the flow in the vicinity of the front is not hydrostatic, it is not governed by the characteristics of shallow-water theory and thus the possibility of a front with constant velocity and depth travelling faster than the maximum characteristic speed is not precluded. For example, with a full-depth release, the energy-conserving half-depth solution away from the front is a valid solution of the shallow water equations, despite the fact that the characteristics are stationary in that case. The shallow-water solution delivers fluid to the non-hydrostatic front, allowing

the front to advance. Support for this picture of non-propagating characteristics is found in our observations (see figures 2 and 11) that the billows in the full-depth release are stationary. We note, however, that if the depth of the flow were to fall below the energy-conserving solution in the hydrostatic flow far from the front, then the behaviour of the characteristics would prevent the half-depth solution being regained, thus explaining our observations of the reduced depth seen with different initial conditions (see figure 10).

We have provided an energy-conserving hydraulic theory for gravity currents produced by lock release. Our theory, although of course an approximation to the flow, is in good agreement with experiments on high-Reynolds-number gravity currents over a wide range of initial lock depths, from shallow locks to full-depth releases. The discrepancies in the observed and predicted velocities are within a few percent and are probably due to losses associated with boundary friction and mixing. Indeed, the effect of the no-slip condition on the lower boundary is to raise the most forward part of the current a small distance from the boundary. This effect can, by itself, reduce the front speed by a few percent. But these losses are not important in describing the order-one dynamics, which are captured by a dissipationless theory.

The reason for the small amounts of dissipation seems clear. As Benjamin (1968) pointed out, potential flow over a semi-infinite current with a flat interface has zero drag. There is probably some form drag associated with the raised head observed on a shallow current but it is small. And, although the mixing looks quite dramatic in shadowgraphs like those shown in figure 2, the extraction of energy from the flow in stratified flows is small. As Linden (1979) shows, mixing is responsible for at most 20–30% of the energy losses in a turbulent flow. Frictional losses at the boundaries are also small for high-Reynolds-number currents.

In deep ambient fluids our theory predicts that the Froude number F_h, based on the current depth h, approaches 1 in the limit of an infinitely deep environment, rather than the larger value of $\sqrt{2}$ predicted by the classical work of von Kármán (1940) and Benjamin (1968). We have carried out new experiments to test the theory and find experimental values for F_h consistent with, but slightly larger than, our predictions. However, the experiments are certainly not consistent with the classical value.

In the limit of an infinitely deep ambient fluid, the only length scale that can be used to define the Froude number is the depth h of the current. As previous experiments and the examples given in this paper show, the value of h depends on the position in the current. The front has a raised head, followed by a region where its depth is a minimum and then it increases again, becoming constant further to the rear of the current. Hydraulic theory assumes that the flow is hydrostatic and requires that it is applied where the current depth is constant. Thus for both Benjamin's and our theory it is necessary that the ends of the control volume be away from the region of the head and the region of minimum depth behind the head. We have chosen to take h as the value at the lock, which lies mid-way between the leftward and rightward propagating disturbances. Previous empirical fits to laboratory data have used a value close to the point of minimum depth behind the head (Huppert & Simpson 1980). This choice gives a larger value for the Froude number, but does not seem to be an appropriate choice for the application of hydrostatic pressure relations. In fact, as Lowe *et al.* (2002) show, vertical velocities are largest in this region. For full-depth releases the depth of the current is almost constant and so the location at which the depth is measured is less problematic.

The present energy-conserving hydraulic theory predicts that the depth of the current at the lock is one-half the initial lock depth D. If instead, single-layer

shallow-water theory is applied, the depth at the lock is $\frac{4}{9}D$. As we show in the Appendix our deep-ambient experiments are slightly closer to this value than $\frac{1}{2}D$ as predicted by the hydraulic theory. We also find that the shallow-water solution conserves energy in this limit.

A further feature that complicates the definition of the current depth is that the interface is, in general, unstable. Benjamin (1968) shows that for a current occupying half the depth, the interface on the top of a heavy current is linearly unstable at all wavelengths. For the light current there is a range of stable wavelengths, which depends on the density ratio γ. For the experiment shown in figure 2(*a*) the interface is stable for wavelengths longer than about $6h$. Even though the density ratio $\gamma = 0.993$ suggests that this flow is Boussinesq, there is a small asymmetry visible, with the light current appearing to be slightly more stable and deeper than the heavy current. Thus our deep-ambient surface current may conform more closely to the hydraulic theory than the more commonly studied dense bottom currents.

Similar values of the Froude number to our experiments were reported by Armi & Farmer (1986) in their study of two-layer exchange flows. When a strong opposing flow produced an arrested current, they predicted and observed a Froude number equal to 1. Although the flows are different since the exchange flow is affected by the changing channel geometry, the agreement in the Froude number value suggests similar dynamics are occurring.

Finally, we note that this approximate hydraulic theory and supporting experiments resolve a number of outstanding questions concerning gravity current dynamics. The theory also provides a closure front condition that can be used in conjunction with shallow-water theory to obtain a more accurate description of the flow than hydraulic theory provides.

Ryan Lowe and James Rottman collaborated on the experiments shown in figures 2 and 8, and we are grateful for their generosity in allowing us to include them in this paper. We have also benefitted enormously from many discussions with them both about gravity currents. We wish to also thank Jake Hacker, James Rottman and Bruce Sutherland for helpful and detailed comments on an early version of this paper. PFL was supported, in part, by the National Science Foundation under Grant No. CTS-0209194. SBD wishes to acknowledge support from the Natural Environment Research Council under grant number NER/A/S/2001/01132.

Appendix. Single-layer shallow-water theory

It is of interest to note some properties of the single-layer shallow-water calculation as a model for a lock release of dense fluid into an infinitely deep environment. Consider a lock, depth D, containing fluid of negative buoyancy g'. The front of the lock is at $x = 0$, and the ambient fluid is infinitely deep. Fluid is released from the lock at $t = 0$. In a variation on the classical St. Venant problem, Abbott (1961) assumed that the front was specified by a constant local Froude number $F_h = U/c = F$, where U is the front speed, $c = \sqrt{g'h}$ and h is the current depth at the leading edge. He showed that

$$U = \frac{2FC}{F+2}, \tag{A 1}$$

where $C = \sqrt{g'D}$. Note that the St. Venant limit of $h = 0$ at the front gives $F \to \infty$ and $U = 2C$.

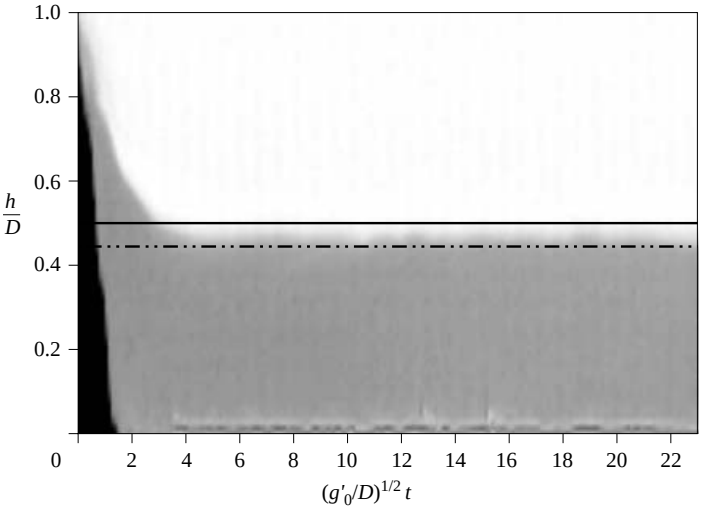

FIGURE 20. The depth of the surface current shown in figure 18 at the lock position plotted against time t. The theoretical value of $\frac{4}{9}$ is shown as the broken line.

The full solution is (see also Klemp *et. al.* 1994)

$$\frac{h}{D} = \begin{cases} 1, & \dfrac{x}{Ct} < 1, \\ \dfrac{1}{9}\left(2 - \dfrac{x}{Ct}\right)^2, & -1 \leqslant \dfrac{x}{Ct} \leqslant \dfrac{2(F-1)}{F+2}, \\ \dfrac{4}{(F+2)^2}, & \dfrac{2(F-1)}{F+2} < \dfrac{x}{Ct} < \dfrac{2F}{F+2}; \end{cases} \tag{A 2}$$

$$\frac{U}{C} = \begin{cases} 0, & \dfrac{x}{Ct} < 1, \\ \dfrac{2}{3}\left(1 + \dfrac{x}{Ct}\right), & -1 \leqslant \dfrac{x}{Ct} \leqslant \dfrac{2(F-1)}{F+2}, \\ \dfrac{2F}{(F+2)^2}, & \dfrac{2(F-1)}{F+2} < \dfrac{x}{Ct} < \dfrac{2F}{F+2}. \end{cases} \tag{A 3}$$

This solution shows that the depth at the lock is $h/D = \frac{4}{9}$, for all values of the front Froude number $F \geqslant 1$. We can compare this with a measured time series of the depth at the lock shown in figure 20. This experiment is the one shown in figure 18, and figure 20 shows the concentration field at the lock position as a function of time. These values give the depth, provided there is no mixing at the lock, which seems a good assumption from the visual observations of the flow shown in figure 18. Figure 20 shows that the depth is very close to the shallow-water prediction, and slightly less than the value 0.5 predicted by the energy-conserving theory given in § 5.

Note that the shallow-water solution (A 2) and (A 3) predicts that the depth and speed of the current are constant behind the front. This region extends back to the lock at $x = 0$ for the case $F = 1$. As discussed in § 9 it seems likely that such a region also exists in the two-layer energy-conserving flow.

It is relevant to examine the energetics of the shallow-water solution. In the following the energies are all per unit width and the density of the fluid is set equal to

unity. The potential energy PE of the current between the front and the rarefaction wave is

$$PE = \frac{1}{2}\rho g' \int_{-Ct}^{\frac{2F}{F+2}Ct} h^2 \,\mathrm{d}x = \frac{3F^5 + 30F^4 + 120F^3 + 240F^2 + 240F + 160}{10(F+2)^5}\rho DC^3 t \quad \text{(A 4)}$$

and the initial potential energy PE_0 of this region is

$$PE_0 = \frac{1}{2}\rho g' \int_{-Ct}^{0} D^2 \,\mathrm{d}x = \frac{1}{2}\rho DC^3 t. \quad \text{(A 5)}$$

The kinetic energy KE of the same region is

$$KE = \frac{1}{2}\rho \int_{-Ct}^{\frac{2F}{F+2}Ct} u^2 h \,\mathrm{d}x = \frac{F^2(F^3 + 10F^2 + 40F + 80)}{5(F+2)^5}\rho DC^3 t. \quad \text{(A 6)}$$

Under the shallow-water approximation the pressure is everywhere hydrostatic, so the front applies a force $\frac{1}{2}\rho g' {h_f}^2$ on the ambient fluid. The motion of the front does work W per unit width

$$W = \frac{16F}{(F+2)^5}\rho DC^3 t. \quad \text{(A 7)}$$

The dissipation ε in the region is equal to the change in potential energy minus the change in kinetic energy and the work done by the front. Using the above expressions we find that $\varepsilon \equiv 0$ for all times. Thus, for a Boussinesq current, energy is conserved by the one-layer shallow-water solution, irrespective of the value of the front Froude number F.

REFERENCES

Abbott, M. B. 1961 On the spreading of one fluid over another. Part II: the wave front. *La Houille Blanche* **6**, 827–836.

Armi, L. & Farmer, D. M. 1986 Maximal two-layer exchange flow through a contraction with net barotropic flow. *J. Fluid Mech.* **164**, 27–51.

Baines, P. G. 1995 *Topographic Effects in Stratified Flows.* Cambridge University Press.

Barr, D. I. H. 1967 Densimetric exchange flows in rectangular channels. *La Houille Blanche* **22**, 619–631.

Benjamin, T. B. 1968 Gravity currents and related phenomena. *J. Fluid Mech.* **31**, 209–248.

Birman, V., Martin, J. E. & Meiburg, E. 2004 The non-Boussinesq lock exchange problem. Part 2. High resolution simulations. *J. Fluid Mech.* (submitted).

Britter, R. E. & Simpson, J. E. 1981 A note on the structure of a gravity current head. *J. Fluid Mech.* **112**, 459–466.

Gardner, G. C. & Crow, I. G. 1970 The motion of large bubbles in horizontal channels. *J. Fluid Mech.* **43**, 247–255.

Härtel, C., Meiburg, E. & Neckar, F. 2000 Analysis and direct numerical simulation of the flow at a gravity current head. Part 1. Flow topology and front speed for slip and no-slip boundaries. *J. Fluid Mech.* **269**, 169–198.

Huppert, H. E. & Simpson, J. E. 1980 The slumping of gravity currents. *J. Fluid Mech.* **99**, 785–799.

von Kármán, T. 1940 The engineer grapples with nonlinear problems. *Bull. Am. Math. Soc.* **46**, 615–683.

Keller, J. J. & Chyou, Y.-P. 1984 On the hydraulic lock exchange problem. *J. Appl. Math. Phys.* **42**, 874–909.

Keulegan, G. H. 1958 The motion of saline fronts in still water. *Natl Bur. Stnd. Rep.* 5813.

Klemp, J. B., Rotunno, R. & Skamarock, W. C. 1994 On the dynamics of gravity currents in a channel. *J. Fluid Mech.* **269**, 169–198.

Linden, P. F. 1979 Mixing in stratified fluids. *Geophys. Astrophys. Fluid Dyn.* **13**, 3–23.

Lowe, R. J., Linden, P. F. & Rottman, J. W. 2002 A laboratory study of the velocity structure in an intrusive gravity current. *J. Fluid Mech.* **456**, 33–48.

Lowe, R. J., Rottman, J. W. & Linden, P. F. 2004 The non-Boussinesq lock exchange problem. Part 1. Theory and experiments. *J. Fluid Mech.* (submitted).

Rottman, J. W. & Linden, P. F. 2001 Gravity currents. In *Stratified Flows in the Environment* (ed. R. H. J. Grimshaw), chap. 4. Kluwer.

Rottman, J. W. & Simpson, J. E. 1983 Gravity currents produced by instantaneous releases of a heavy fluid in a rectangular channel. *J. Fluid Mech.* **135**, 95–110.

Shin, J. O. 2002 Colliding gravity currents. PhD thesis, University of Cambridge.

Simpson, J. S. 1997 *Gravity currents in the environment and the laboratory*, 2nd Edn. Cambridge University Press.

Simpson, J. E. & Britter, R. E. 1979 The dynamics of the head of a gravity current advancing over a horizontal surface. *J. Fluid Mech.* **94**, 477–495.

Turner, J. S. 1973 *Buoyancy Effects in Fluids*. Cambridge University Press.

Wilkinson, D. L. 1982 Motion of air cavities in long horizontal ducts. *J. Fluid Mech.* **118**, 109–122.

Yih, C. S. 1947 A study of the characteristics of gravity waves at a liquid interface. MS Thesis, State University of Iowa.

Yih, C. S. 1965 *Dynamics of Nonhomogeneous Fluids*. Macmillan.